Article

Escherichia coli ST648 Chronically Infecting Patients with Cystic Fibrosis. An Approach to Eradication

Olga L. Voronina *, Marina S. Kunda, Natalia N. Ryzhova, Ekaterina I. Ermolova, Elizaveta R. Goncharova, Ekaterina A. Koroleva, Lidia N. Kapotina, Elena Yu. Morgunova, Elena L. Amelina, Nailya A. Zigangirova

Posted Date: 4 August 2025

doi: 10.20944/preprints202508.0234.v1

Keywords: Cystic fibrosis; *Escherichia coli* ST648; AMR; virulence factors; plasmids; transposons; Fluorthiazinon

 doi:10.20944/preprints202508.0234.v1

Article

Escherichia coli ST648 Chronically Infecting Patients with Cystic Fibrosis: An Approach to Eradication

Olga L. Voronina [1,*], Marina S. Kunda [1], Natalia N. Ryzhova [1], Ekaterina I. Ermolova [1], Elizaveta R. Goncharova [1], Ekaterina A. Koroleva [1], Lidia N. Kapotina [1], Elena Yu. Morgunova [1], Elena L. Amelina [2] and Nailya A. Zigangirova [1]

[1] N.F. Gamaleya National Research Center for Epidemiology and Microbiology, Ministry of Health of Russia; Gamaleya Str., 18, 123098 Moscow, Russia

[2] Pulmonology Research Institute under FMBA of Russia, Orekhovy Boulevard, 28, building 10, 115682, Moscow, Russia

* Correspondence: olv550@gmail.com

Abstract

Extraintestinal pathogenic *Escherichia coli* causes community-acquired and nosocomial pneumonia, and poses a risk of infection, especially for patients with impaired lung function, such as patients with cystic fibrosis (CF). When chronic infection develops, eradication of the pathogen is difficult even with aggressive antibacterial therapy and targeted CF treatment. A new compound, Fluorthiazinone (CL-55), an inhibitor of bacterial virulence, was registered in Russia in 2024. The aim of our study was to characterize the genomes of *E. coli* ST648 isolated from long-term infected CF patients, describe AMR and virulence factors, and investigate the effect of CL-55 on CF isolates in vitro. Comparison of the genomes of hypermucoviscous isolates showed that, in the presence of a large number of core genes, the isolates have adaptive differences both in chromosome and in the composition and genes of the plasmidome. Both isolates formed mature biofilms on an abiotic surface and were able to survive and proliferate inside macrophages. CL-55 in in vitro experiments was effective in suppressing *E. coli* ST648 in both the aggregate and intracellular states, which allows us to propose the use of Fluorothiazinone as a combinative therapy to facilitate eradication of pathogenic microorganisms in the respiratory tract of patients with CF.

Keywords: Cystic fibrosis**;** *Escherichia coli* ST648; AMR; virulence factors; plasmids; transposons; Fluorthiazinon

1. Introduction

Extraintestinal pathogenic *E. coli* (ExPEC) is one of the pathogens found in patients with respiratory infections and sepsis, and has been reported in the cases of community-acquired (CAP), nosocomial (NP), and especially ventilator-associated pneumonia (VAP) [1,2]. The proportion of patients with pneumonia caused by *E. coli* varies from 7.7% in CAP in the USA [3] to 19% in VAP in France [4]. For Germany VAP cases, *E. coli* was the dominant isolate [5]. *E. coli* causing pneumonia in 55% of cases belong to the phylogenetic group B2 [4], for example, to the pandemic ExPEC ST131 clonal lineage [6]. Another international high-risk clonal lineage ST648, belonging to phylogenetic group F, is young, nascent, characterized by low genetic diversity and association of carriage of antimicrobial resistance (AMR) genes with increased virulence potential [7]. It should be noted that according to the assessment of the global burden of AMR from 1990 to 2021, *E. coli* was among the top three causes of deaths among adults and children after *Staphylococcus aureus*, *Acinetobacter baumannii* due to resistance to aminopenicillins, beta-lactams and beta-lactamase inhibitors, fluoroquinolones, 3rd generation cephalosporins [8].

 doi:10.20944/preprints202508.0234.v1

The spread of pathogenic *E. coli* lineages increases the likelihood of acquiring infection from the environment, in the community, and in hospitals by patients from risk groups, such as patients with cystic fibrosis (CF). CF is a chronic genetic disorder caused by a mutation in the gene of the CF transmembrane conductance regulator (*cftr)*, and leading to systemic pathology. Chronic lung infections are important manifestations of CF, causing progressive airways disease and, respiratory failure - the primary cause of mortality of CF patients [9]. *E. coli* is not a classical CF pathogen, which is probably why the CF registries of European countries and the USA do not register the data on chronic *E. coli* infection. However, some information is available in scientific literature. A seven-year-long study of 176 CF patients in two German CF centers revealed 11% of the *E. coli* chronically infected patients [10]. In Canada, over 38 years of observation of 366 CF patients, the proportion of *E. coli* chronically infected patients was 4.9%, and 2.4% of patients experienced exacerbation due to *E. coli* infection [11,12]. In the Moscow region, according to the registry of Russian patients with CF, the proportion of patients with chronic lung *E. coli* infection was 3.6% in 2023 [13]. In our study of the lung microbiome of 50 adult CF patients from the Moscow region, three patients had chronic *E. coli* infection. Two patients were infected with *E. coli* ST648, and one patient - with *E. coli* ST1193.

Long-term persistence and difficulties in eradication of *E. coli* are associated with the genetic characteristics of ExPEC strains, with those responsible for the virulence potential, in particular. One of the especially important virulence determinants is the capsular polysaccharide (CPS), or K antigen. K antigens have been classified into four groups [14]. ExPEC associated with invasive disease usually express group 2 CPS that includes K1, K4, K5 polysaccharides, et al. [15]. The expression of this group of CPS is temperature-regulated and is switched on inside the host at 37°C [14]. ExPEC strains producing group 2 CPS may also co-express colanic acid. Excessive production of these surface polysaccharides can result in a hypermucoviscous phenotype [16]. It has been shown that the hypermucoviscosity of *K. pneumoniae* isolates has also been associated with the development of invasive syndrome [17]. Some exceptional hypermucoviscous ExPEC strains have been described [16,18]. The hypermucoviscous phenotype decreases the immunological host defenses and enhances the bacterial survival rates [19].

E. coli infection is initiated by bacterial adhesion to the lung epithelial surface. Direct interactions between human interleukin-8 (IL-8) and the chemoreceptor Tsr expressed on the surface of *E. coli* play an important role in the transmigration of the bacterium across the human lung mucosal barrier via both paracytosis and transcytosis [20]. Several in vitro (cell culture) and in vivo (in mice) studies have shown that *E. coli* is able to invade alveolar epithelial cells type II [21], to persist in macrophages [22,23], and neutrophils [24]. As a result, the presence of AMR and virulence factors, the ability to form biofilms and persist within different types of eukaryotic cells allow *E. coli* to avoid the effects of maintenance and episodic antibiotic, and CFTR-modulator therapy.

A new compound, Fluorthiazinone (C19H17F2N3O4S; FT), which is an inhibitor of bacterial virulence, was registered in Russia in 2024 to be used to treat patients with complicated urinary tract infections in combination with antibiotics [25]. FT specifically inhibited the type 3 secretion system (T3SS) and flagella of Gram-negative bacteria and was effective in the suppression of model infections caused by different pathogenic bacteria of the kingdom *Pseudomonadati* [25].

So, the aim of our study was to compare the genomes of isolates obtained from two patients with *E. coli* ST648, describe AMR and virulence factors, and investigate the effect of FT on *E. coli* ST648 isolated from long-term infected CF patients in vitro to evaluate the impact of FT on characterized isolates.

2. Results

2.1. Microbiome of the Sputum Samples

The sputum samples of the long-term E. coli infected patients 119-CF and 149-CF were analyzed for the presence of E. coli by amplification and sequencing of 16S rDNA and adk gene fragments. The main pathogen was E. coli, and the proportion of E. coli, according to the analysis of the microbiome

 doi:10.20944/preprints202508.0234.v1

composition, was 91 and 90% in the samples of patients 119-CF and 149-CF, respectively (Figure 1). Streptococcus and Prevotella were present in small quantities in the 119-CF microbiome, and Pseudomonas and Trabulsiella were present in the 149-CF microbiome. These samples were used for E. coli isolation. The isolates GIMC1402:EC_33P15 (patient 119-CF) and GIMC1403:EC_33P43 (patient 149-CF) were primarily characterized using whole genome sequencing.

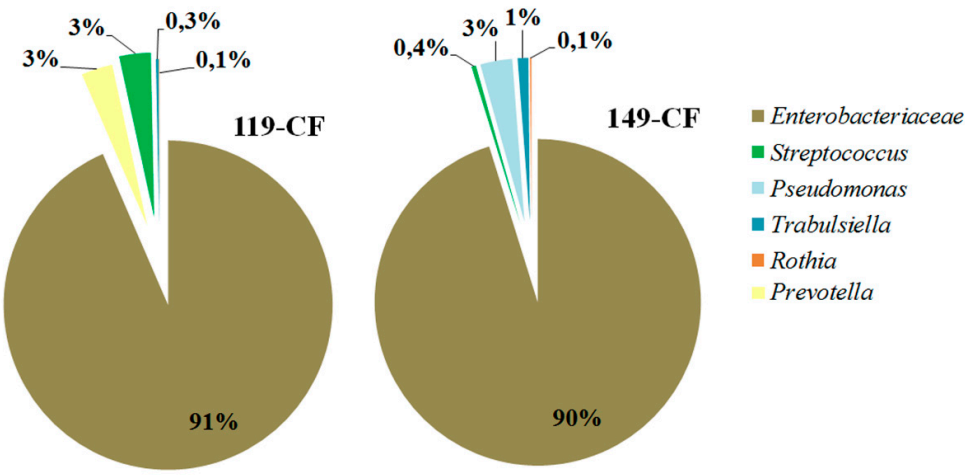

Figure 1. Microbiome composition of sputum samples from which *E. coli* GIMC1402:EC_33P15 (patient 119-CF) and GIMC1403:EC_33P43 (patient 149-CF) were isolated.

2.2. Features of the Genomes of E. coli Isolates

Genomic analysis of isolates GIMC1402:EC_33P15 and GIMC1403:EC_33P43 showed that both isolates belonged to the phylogenetic group F, the international high-risk clone ST648, and had antigen profiles O153:H6:K5 (GIMC1402:EC_33P15) and O153:H6:K4 (GIMC1403:EC_33P43).

The main features of genome annotation are presented in Table 1. The GIMC1402:EC_33P15 chromosome is large than the GIMC1403:EC_33P43 one, contains more CDSs (Coding DNA Sequences) and pseudogenes. Both genomes contain extrachromosomal DNA elements, represented by plasmids and phage-plasmids. The biggest are plasmids 1 and phage-plasmids with a size of more than 100 kb, which are present in 1 copy per cell. The small plasmids with sizes of 2.1 – 7.2 kb have copy numbers of 10 – 20 per cell. All small plasmids encode Rep initiator proteins; some of them encode proteins required for conjugal mobilization, and virulence factors, for example, minor pilin of the type IV secretion complex, VirB5.

Table 1. Main features of genome annotation of *E. coli* isolates.

Features	GIMC1402:EC_33P15	GIMC1403:EC_33P43
Chromosome, bp.	5115804	5032495
Genes (total)	5292	5154
CDSs (total)	5171	5032
Genes (RNA)	121	122
tRNAs	94	95
Pseudo Genes (total)	206	202
CRISPR Arrays	2	2
Plasmid	pEC_33P15-1 (134688 bp) pEC_33P15-2 (4237 bp)	pEC_33P43-1 (110734 bp) pEC_33P43-2 (7176 bp)

 doi:10.20944/preprints202508.0234.v1

	pEC_33P15-3 (4072 bp)	pEC_33P43-3 (2091 bp)
		pEC_33P43-4 (1459 bp)
Phage-Plasmid	p-pEC_33P15 (108306 bp)	p-pEC_33P43 (107320 bp)

2.2.1. Phage-Plasmids

Phage-plasmids (P-P) had dual functionality: they can replicate independently as plasmids and carry prophage sequences. Under specific conditions, a release of intact phage could occur, which may lead to bacterial cell infection and death. P-Ps of the isolates GIMC1402:EC_33P15 and GIMC1403:EC_33P43 belong to the plasmid incompatibility group IncFIB. On the basis of the genome-wide sequence similarity, these P-Ps are a part of a super community SSU5 of phage-plasmids that are associated with species of the *Enterobacteriaceae* family, and belong to the pSLy3 group according to the classification of Pfeifer et al. [26]. Phage-plasmids contain intact prophage sequences of 76.2 kb in length (Figure 2), *repB* gene for plasmid replication initiator protein; but don't carry any genes encoding AMR. It is interesting that both P-P acquired the *apbC* gene for iron-sulfur cluster carrier protein ApbC. ApbC could bind and rapidly transfer iron-sulfur ([Fe-S]) clusters to an apoprotein and, in addition, has ATPase activity. ApbC is a member of the ParA subfamily of proteins that have a wide array of functions, including electron transfer, initiation of cell division, and DNA segregation [27].

2.2.2. The Large Plasmids pEC_33P15-1 and pEC_33P43-1

The large plasmids of the isolates are characterized by IncFIB/IncFII/IncFIA and belong to the F family of the conjugative plasmids. Complete nucleotide sequence comparison of pEC_33P15-1 and pEC_33P43-1 revealed regions of homology, three inverted regions, and regions of difference (Figure 3). The main regions of difference contained transposons and class 1 integron that were present only in plasmid pEC_33P15-1. The regions included the following genes: *tet(B)* and *tetR(B)* (resistance to tetracyclines), *catA1* (chloramphenicols), *mph(A)* and *mrx(A)* (macrolides), *sul1* (sulfonamides), *qacE* (quaternary ammonium compounds), *aadA5* (aminoglycosides), and *dft17* (trimethoprim) (Table 2). The genes acquired by plasmid enhance the potential for resistance of isolate GIMC1402:EC_33P15 to different classes of antimicrobial drugs.

 doi:10.20944/preprints202508.0234.v1

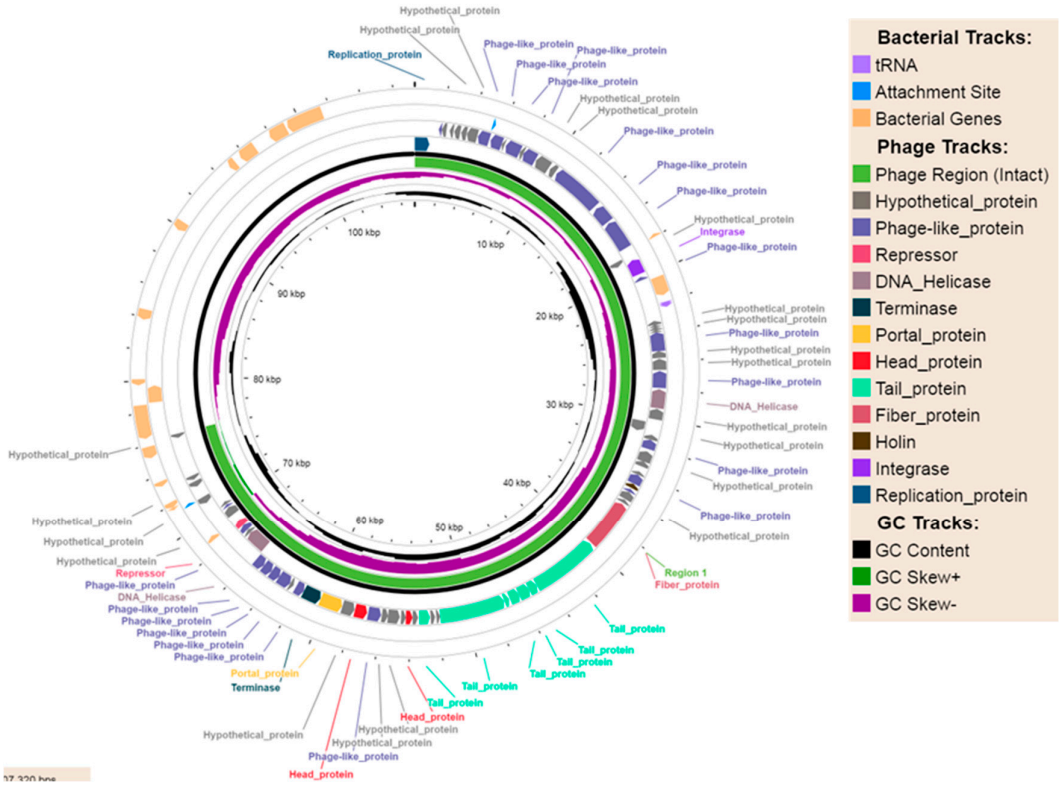

Figure 2. Phage-plasmid episome as part of the genomes of E. coli isolates GIMC1402:EC_33P15 and GIMC1403:EC_33P43.

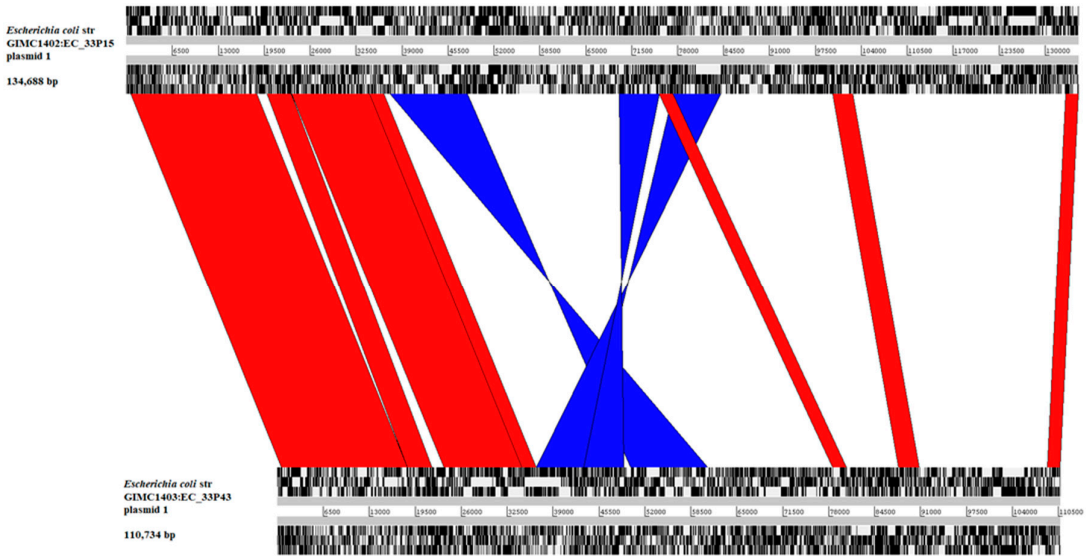

Figure 3. Complete DNA sequence plasmid comparisons.

Upper scale - plasmid pEC_33P15-1 of isolate GIMC1402:EC_33P15, lower scale - plasmid pEC_33P43-1 of isolate GIMC1403:EC_33P43. Bands of color indicate homology between sequences. Red lines show sequence in the same confirmation; blue lines indicate sequence inversion.

 doi:10.20944/preprints202508.0234.v1

Table 2. Resistance and virulence factors in pEC_33P15-1 and pEC_33P43-1.

Category	Function		GIMC1402:EC_33P15, pl1	GIMC1403:EC_33P43, pl1
			Product (genome position)	Product (genome position)
Resistance	Tetracycline resistance		tetracycline efflux MFS transporter Tet(B) (50012..51217)	–
			transcriptional repressor TetR(B) (51299..51922)	–
	Chloramphenicol resistance		CatA1, chloramphenicol O-acetyltransferase (54209..54868)	–
	Macrolide resistance		Mph(A), family macrolide 2'-phosphotransferase (59909..60814)	–
			Mrx(A), macrolide resistance MFS transporter (60811..62049)	–
	Sulfonamide resistance		Sul1 sulfonamide-resistant dihydropteroate synthase (66125..66964)	–
	Aminoglycoside resistance		AadA5, ANT(3")-Ia family aminoglycoside nucleotidyltransferase (67511..68299)	–
	Trimethoprim resistance		Dft17, trimethoprim-resistant dihydrofolate reductase (68430..68903)	–
	Quaternary ammonium compound resistance		QacE, QAC efflux SMR transporter (66958..67305)	–
Virulence factors	Protection against the macroorganism's compliment system; participation in the biofilm formation		the F-type transfer system (24233 – 34796; 79117 – 84085)	the F-type transfer system (22132 - 41597)
	Colonization and survival under conditions of Fe2+, Pb2+, Zn2+ and Mn2+ deficiency		iucABCD, iutA, aerobactin (110608..119908)	–
			Fe^{2+} ABC-transporter (38945..43430)	Fe^{2+} ABC-transporter (59262..54777)
			Fe^{2+}/Pb^{2+} ILT-transporter (43534..45988)	Fe^{2+}/Pb^{2+} ILT-transporter (54673..52237)
			SitABCD ABC-transporter (105156..108605)	–
			–	TonB-dependent transport system (68082..71288; 81969..83939)
			–	YncE protein (71357..72532)
Toxin-antitoxi	Selective advantage of a clone in a bacterial	Type I*	Mok/Hok TA (20002..20218)	Mok/Hok TA (18537..18753)
			Hok/Gef TA (77769..77903)	Hok/Gef TA (42811..42945)

 doi:10.20944/preprints202508.0234.v1

	population, formation of a persistent cell population	Type II**	–	Phd_YefM/ Fic_DOC TA (98859..99460)
			VapB/VapC TA (123886..124529; 128749..129392)	–
			CcdA/CcdB TA (133356..133881)	CcdA/CcdB TA (109402..109927)
			PemL/PemK TA (71821..72412)	PemL/PemK TA (46343..46934)

* The antitoxin is a small antisense RNA targeting toxin mRNA for degradation and/or inhibition of translation [28]. ** The antitoxin is a protein that forms a stable inactive complex with the toxin [28].

Analysis of virulence factors (Table 2) revealed the presence in both plasmids some genes encoding the proteins that increase survival under conditions of deficiency of divalent metal ions. These are ABC (ATP-binding cassette) - and ILT (iron/lead transporter) -transport systems that ensure efficient iron capture under conditions of limited iron availability, which contributes to the virulence and competitiveness of GIMC1402:EC_33P15 and GIMC1403:EC_33P43 isolates. In addition, ABC transporters are involved in the secretion of virulence factors and promote bacterial survival by efflux of toxic xenobiotics, which in turn contributes to antimicrobial resistance [29]. Aerobactin (*iucABCD*, *iutA*) clusters responsible for the synthesis of the siderophore that enables the capture and transport of iron from the environment, as well as the *sitABCD* transporter, were identified only in pEC_33P15-1. The *sitABCD* operon encoded an ABC transporter that transports divalent Fe^{2+} and Mn^{2+} cations, which not only promotes metal uptake but also enhances the resistance of the bacterium to oxidative stress. In addition, the *sitABCD* operon and the *qacE* gene identified in pEC_33P15-1 provide resistance to disinfectants [30,31]. Genes for aerobactin were absent in pEC_33P43-1. However, this plasmid carried *yncE* gene and gene encoded TonB-dependent metal ion transport system, that were absent in pEC_33P15-1.

One more important virulence factor is the F-type transfer system, represented by several *tra* and *trb* genes, and by *finO* gene, which are gathered in one 19.465 kb region in plasmid pEC_33P43-1. In plasmid pEC_33P15-1, this gene region is divided into 2 parts: 10563 and 4968 kb, due to recombination and inversion. The F-type transfer system encodes the proteins involved in the elaboration of the conjugative pilus and the T4SS (type 4 secretion system) required for the formation of the mating pair, as well as the relaxosome components needed for the processing of the plasmid prior to transfer [32]. But first of all, what is interesting is the pilin TraA, which is the main adhesion factor that induces biofilm formation in addition to flagella, type 1 fimbriae, Ag43, and curli, which are essential to *E. coli* biofilm [32]. So, the conjugative pilus itself of a derepressed F plasmid can promote the biofilm of *E. coli* cells [33]. Moreover, the F plasmid, which does not express F pili, can induce the production of curli, which affects the maturation of the three-dimensional structure of the biofilm [34]. Another mechanism of enhancing biofilm formation under the influence of plasmids is mediated by their effect on reducing motility and increasing the level of quorum-sensing inducer AI-2 (auto inducer 2) [35]. Thus, the entire set of episomes contributes to biofilm formation by GIMC1402:EC_33P15 and GIMC1403:EC_33P43 isolates.

The next group of factors are the toxin-antitoxin systems. Two toxin-antitoxin systems type I (Mok/Hok, Hok/Gef) and two systems type II (CcdA/CcdB and PemL/PemK) are common for both plasmids (Table 2). Type II toxin-antitoxin system VapB/VapC is unique to pEC_33P15-1, and Phd_YefM/Fic_DOC system is unique to pEC_33P43-1. The main function of toxin-antitoxin systems is to ensure the stability of plasmid inheritance and the formation of persister cells [36]. The presence of toxin-antitoxin determines the selective advantage of a clone in the bacterial population and the formation of a stable cell population. Thus, thanks to the plasmid, isolate GIMC1402:EC_33P15 is characterized by more pronounced antibiotic resistance and an expanded set of virulence factors, which may provide it with advantages in antibiotic therapy and intermicrobial competition, whereas GIMC1403:EC_33P43 shows less potential for drug resistance.

 doi:10.20944/preprints202508.0234.v1

2.2.3. Comparative Analysis of Chromosomes

Comparative analyses of chromosomes revealed some regions of differences (Figure 4). First of all, they were associated with mobile genetic elements (MGE): prophages (Figure 4) and transposons (Table 3). Two regions of transposons containing AMR determinants are presented in Table 3. Region 2, which includes the CTX-M-15 beta-lactamase ORF (open reading frame), is identical in isolates. Region 1 contains ORFs present in both genomes (for aminoglycoside acetyltransferase AAC(6')-Ib-cr and beta-lactamase OXA-1) and ORFs distinctive for GIMC1402:EC_33P15: for aminoglycoside acetyltransferase AAC(3)-IIa, beta-lactamase TEM-1, and for gene of the tunicamycin resistance protein TmrB. Region 1 is partly included in Indel 1 (Figure 4). In addition, Indel 1 contains the operon for ABC transporter complex UgpBAEC involved in import of sn-glycerol-3-phosphate (G3P), which is missing in GIMC1403:EC_33P43. G3P is an important intermediate in the lipid biosynthesis, and is a carbon source [37].

Table 3. Transposon regions containing AMR genes.

	GIMC1402:EC_33P15		**GIMC1403:EC_33P43**	
Region	**Gene**	**Product**	**Gene**	**Product**
1	351708..350878	TEM-1		
	351852..352556	IS6-Tnp	331206..331280	IS6-Tnp-pseudo
	352700..353254	AAC(6')-Ib-cr	331424..331978	AAC(6')-Ib-cr
	353385..354215	OXA-1	332109..332939	OXA-1
	354353..354793	CatB3-pseudo	333077..333517	CatB3-pseudo
	complement(354847..355551)	IS6-Tnp	complement(333571..334275)	IS6-Tnp
	355658..356518	AAC(3)-IIa		
	356531..357073	tmrB		
	357165..358213	IS3-Tnp		
	complement(358267..358971)	IS6-Tnp		
2	complement(359039..361267)	Tn3-Tnp-pseudo	complement(334343..336571)	Tn3-Tnp-pseudo
	complement(361672..362547)	CTX-M-15	complement(336976..337851)	CTX-M-15
	complement(362803..364065)	IS1380-Tnp	complement(338107..339369)	IS1380-Tnp

Indel 2 contains 4 ORFs that are specific to GIMC1402:EC_33P15, including the ORF of the small membrane protein Blr, which is capable of interacting with several divisomal proteins and stabilize their assembly into a functional machinery [38]. This characteristic is also shared by YmgF, which is present in both isolates. However, an additional function of Blr is to increase the *E. coli* cell's resistance to a wide spectrum of beta-lactam antibiotics or other drugs that inhibit peptidoglycan synthesis [39].

Indel 3 was formed as a result of duplications and recombination of individual regions in the chromosome of GIMC1402:EC_33P15. For example, ORFs for the type IV toxin-antitoxin system are repeated three times in the GIMC1402:EC_33P15 genome, while in the GIMC1403:EC_33P43 genome they are present in one copy.

The marker operon for Indel 4 is the operon for the tripartite ATP-independent periplasmic (TRAP) transporter, which uses energetically favorable cation gradients to drive the import of specific carboxylate- and sulfonate-containing nutrients against their concentration gradient [40]. Thus, in the GIMC1403:EC_33P43 genome there are three TRAP operons, and in the GIMC1402:EC_33P15 genome there are only two operons.

 doi:10.20944/preprints202508.0234.v1

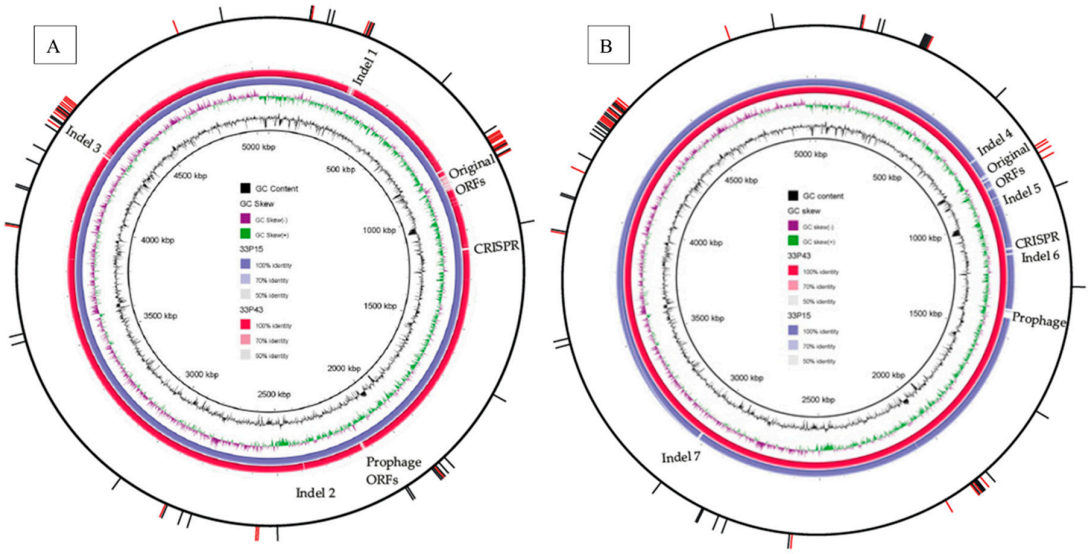

Figure 4. Comparative analysis of chromosomes of E. coli isolates GIMC1402:EC_33P15 and GIMC1403:EC_33P43. 1-7 - numbers of regions of differences. A) The query is GIMC1402:EC_33P15; B) the query is GIMC1403:EC_33P43.

Indel 5 includes ORFs of the energy-coupling factor (ECF) - ABC transporter for cobalt transport. This operon is absent in the GIMC1402:EC_33P15 genome.

Indel 6 gathers genes for some metabolic pathways and for additional GntP family transporter (gluconate:H+ symporter), and is missing in the GIMC1402:EC_33P15 genome.

Indel 7 includes 11 ORFs lacking in GIMC1402:EC_33P15. The most important of these for describing resistance and virulence factors are *mdtH* gene encoding multidrug efflux MFS transporter, and biofilm formation regulator BssS. BssS, being a component of the GlaR regulon, is itself involved in the regulation of indole, and uptake and export of AI-2 through a cAMP-dependent pathway, so BssS regulates biofilm through signal secretion [41].

Another indel is related to differences in the sequences of the CRISPR-Cas regions (Table 4). Both regions of the strain GIMC1402:EC_33P15 have the same repeat sequences but different numbers of spacers, so the CRISPR regions have different lengths and belong to different IDs according to the CRISPR database. CRISPR regions of the strain GIMC1403:EC_33P43 differ in both repeat sequences and the number of spacers. One of the regions has the same ID as the CRISPR region of strain GIMC1402:EC_33P15, the other had no analogues in the database. In general, the length of the CRISPR regions in the genome of this strain was less than that of GIMC1402:EC_33P15. The sequences of the eight Cas protein genes were identical except for one encoding Cas 3.

Table 4. CRISPR in *E. coli* genomes.

Position	CRISPR Length	Consensus_Repeat	Repeat ID (CRISPRdb)	Spacers Nb	Evidence Level
GIMC1402:EC_33P15					
1154150…1155279	1129	GTGTTCCCCGCGCCAGCGGGGATAAACCG	R6121	18	4
1180826…1181648	822	GAGTTCCCCGCGCCAGCGGGGATAAACCG	R3946	13	4
GIMC1403:EC_33P43					
1115575…1116213	638	GAGTTCCCCGCGCCAGCGGGGATAAACCG	R3946	10	4
1143351…1143925	574	GTGTTCCCCGCGCCAGCGGGGATAAA	Unknown	9	4

 doi:10.20944/preprints202508.0234.v1

The biggest one was the region of original ORFs (Figure 4). The formation of such a region was determined by differences in the K loci (Figure 5). The K loci of both strains belong to group 2, include conserved regions 1 and 3, and serotype-specific region 2. According to the structure of region 2, K5 strain GIMC1402:EC_33P15 and K4 strain GIMC1403:EC_33P43 synthesize a (GlcA-GlcNAc)n and a (GalNAc-GlcA(Fru))n polymers, respectively.

The second cluster of genes in the region of original ORFs encodes proteins for the metabolosome (bacterial microcompartment) organization and enzymes for propanediol utilization. GIMC1402:EC_33P15, containing this operon, benefits from the ability to utilize alternate carbon sources under conditions of inflammation.

Thus, a comparison of the chromosomes of two *E. coli* ST648 isolates showed that, despite the large number of core genes, the isolates differ in antigenic, metabolic, virulence, and resistance characteristics, reflecting the processes of adaptation of each isolate to the peculiarities of the respiratory tract of a particular patient.

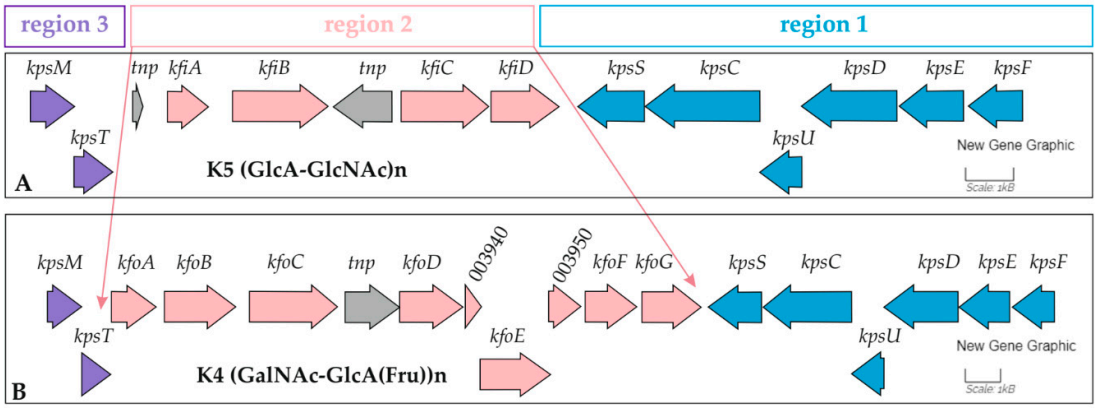

Figure 5. Organization of the genes required for the synthesis of K5 (A) and K4 (B) capsules. Regions 3 (violet) and 1 (blue) flanked the region 2 (pink). ORFs of the transposases are colored grey.

The evidence of numerous introductions into genomes of GIMC1402:EC_33P15 and GIMC1403:EC_33P43 isolates is the presence of a large number of both functioning genes (40 and 32) and pseudogenes (24 and 30) of transposases. Most of them (51 and 49) were identified as transposases of 15 IS families. IS3, IS1, IS66 were predominant. One of such introductions resulted in the acquisition of the CTX-M-15 gene, which was important for the evolution of *E. coli* ST648.

2.2.4. The Place of CF Isolates in the Population Structure of *E. coli* ST648

The carriage of extended-spectrum beta-lactamase (ESBL) genes, especially CTX-M, is the hallmark of *E. coli* ST648. The strains of CF patients produced CTX-M-15 belonging to the CTX-M-1 group. CTX-M-15 was first observed in 1999 in the isolate from India, and now it is widespread over the world [42]. To roughly determine the time of infection of CF patients, we used the results of the analysis of the population structure of *E. coli* ST648, performed by Schaufler et al. for 87 strains isolated between 2006 and 2014 in different countries of the world [7]. The authors estimated that the earliest clades 3 and 4 separated from the latest clades 1 and 2 in 2004. The strains of the clades 3 and 4 carried CTX-M of the different alleles. The strains with CTX-M-15 belonged to the clades 2 and 1. The split of the clades 1 and 2 occurred in 2006.

We performed a pairwise alignment of the genomes of CF isolates and strains- representatives of clades 1-4 to calculate the ANI and AP values (Table 5). As follows from the data in Table 5, the ANI values were in the range of 98.84 - 99.72, which characterized an extremely closely related group of isolates within the species. According to the ANI and AP values, CF strains belonged to the latest clade 1 formed in 2006, therefore, with a certain degree of probability, the infection of patients

 doi:10.20944/preprints202508.0234.v1

occurred no earlier than 2006. The first molecular genetic confirmation of the genotype of *E. coli* infecting CF patients was obtained in 2013 for patient 119-CF and in 2015 for patient 149-CF.

Table 5. The pairwise ANI (Average Nucleotide Identity) and AP (Alignment Percentage) values between study isolates and strains-representatives of the clades 1-4 for *E. coli* ST648.

Strain, Accession number	GIMC1402:EC_33P15, CP181181.1	GIMC1403:EC_33P43, CP181392.1	NA023, JSXK000000000.1	32 - 2823 ED, DABAXP000000000.1	VB 962116, DABAMI000000000.1	F_30_1_R8, PIIR000000000.1
clade			1	2	3	4
GIMC1402:EC_33P15	-	99,61	**99,49**	**99,54**	98,92	99,08
GIMC1403:EC_33P43	95,65	-	**99,39**	**99,36**	98,84	98,98
NA023, clade 1	**92,45**	**91,54**	-	99,51	98,98	98,98
32 - 2823 ED, clade 2	89,32	89,96	90,07	-	99,33	99,43
VB 962116, clade 3	88,07	87,82	98,98	90,01	-	99,72
F_30_1_R8, clade 4	90,63	89,98	89,95	89,76	90,87	-

The upper right triangle shows the ANI values (%), the lower left triangle shows the AP values (%). The *E. coli* ST648 clades were determined according to Schaufler et al. [7].

2.2.5. Adaptation to the Long-Term Chronic Infection

Long-term persistence in the airways during inflammation has formed a hypermucoviscous phenotype of CF isolates (Figure 6). Colanic acid (CA) is the major exopolysaccharide produced by *E. coli*. CA forms slime, which increases cell viability and protects bacterial cells from environmental stress [43]. Up-regulation of the CA production is promoted by the global regulators LsrF and LsrK bound with AI-2. The production of the CA is a part of the process of colonization. In addition to colonization, AIs also promote aggregation, biofilm formation, and adherence. KEGG pathway maps approved the presence of functional genes for the indicated processes in CF isolates (Figure 7).

 doi:10.20944/preprints202508.0234.v1

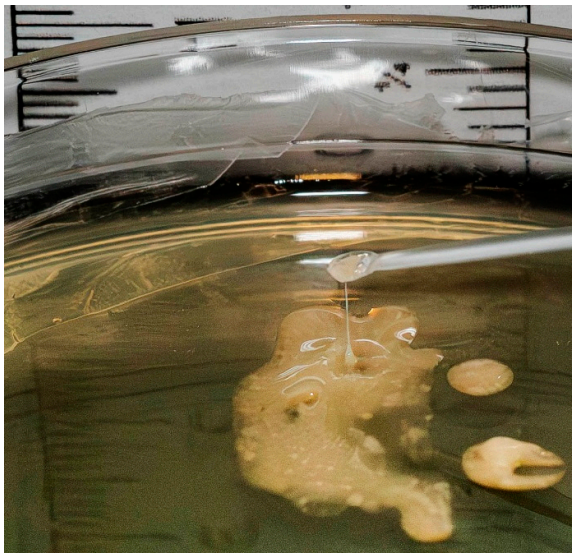

Figure 6. The hypermucoviscous colonies of the GIMC1402:EC_33P15 strain cultivated on LB agar.

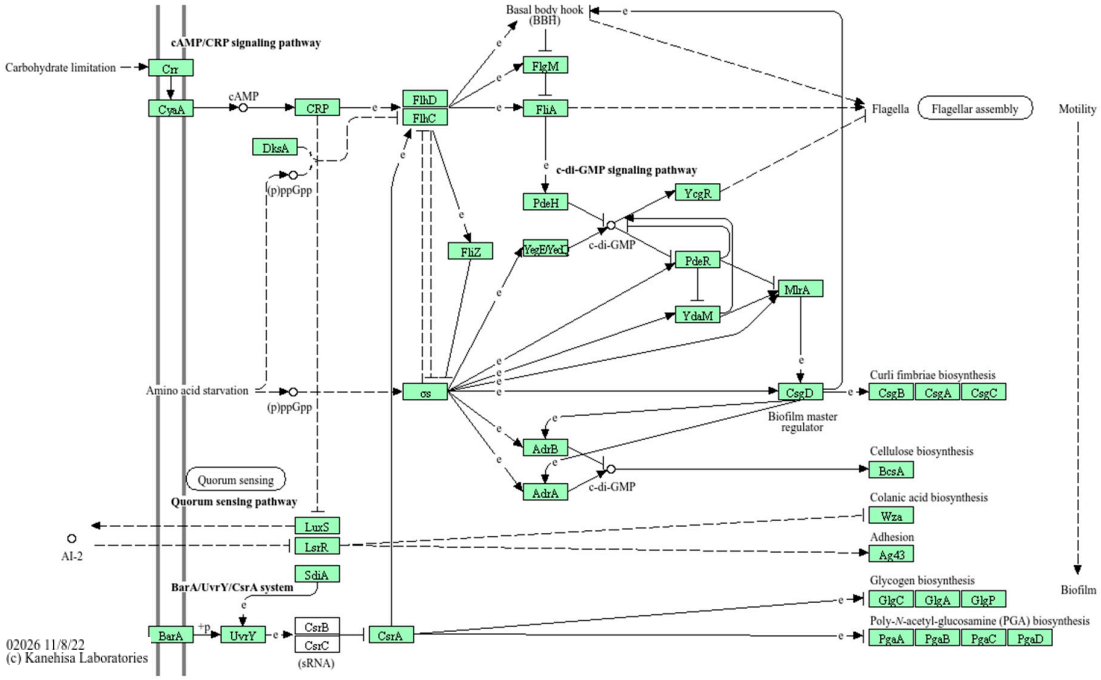

Figure 7. Pathways for biofilm formation. Functional genes in the genome of isolate GIMC1402:EC_33P15 are highlighted in green.

As shown by BlastKOALA analysis, CF isolates could synthesize, export extracellularly, and internalize AI-2 and AI-3. The role of AI-2 in the biofilm formation is shown in Figure 7. AI-3, in turn, via the QseBC system, regulates the expression of flagella and controls the formation of biofilm, influencing its thickness and architecture.

The next strategy for bacterial survival during chronic infection is to hijack and overcome the host's antimicrobial responses and to overcome the effects of antibiotics used for treatment. This is realized by invading epithelial cells and macrophages for survival and replication. This is facilitated by two secretion systems: type 3 (T3SS) and type 6 (T6SS). The genomes of CF isolates contain T3SS, named by Hayashi et al. *E. coli* type 3 secretion system 2 (ETT2) [44]. The genes of the two regions encode components of the secretion apparatus. The EspL1 effector gene is located separately. The T6SS genes, with the exception of the genes encoding the tip protein VgrG, are concentrated in one

 doi:10.20944/preprints202508.0234.v1

chromosome cluster. The cluster includes, among other things, the *hcp1* and *hcp2* genes encoding the T6SS effectors.

We assessed the ability of isolates to invade and replicate in macrophages, as well as the efficiency of biofilm formation, in in vitro experiments.

2.3. In Vitro Experiments

2.3.1. Biofilm Formation

Both isolates grew slowly due to the previously noted hypermucoviscous nature, which is consistent with the observation of Cui et al. that virulent pathogens grow slower because they can divert more energy towards other disease-specific processes, such as the production of virulence factors [45]. Therefore, the observation time for the ability of *E. coli* isolates to form biofilms on an abiotic surface of the 96-well plates was longer. After cultivation for 72 hours, both isolates formed typical mature biofilms (Figure 8). However, the biofilm of the GIMC1403:EC_33P43 isolate was significantly denser according to the determination of biomass (Figure 8) and matrix staining (Figure 9).

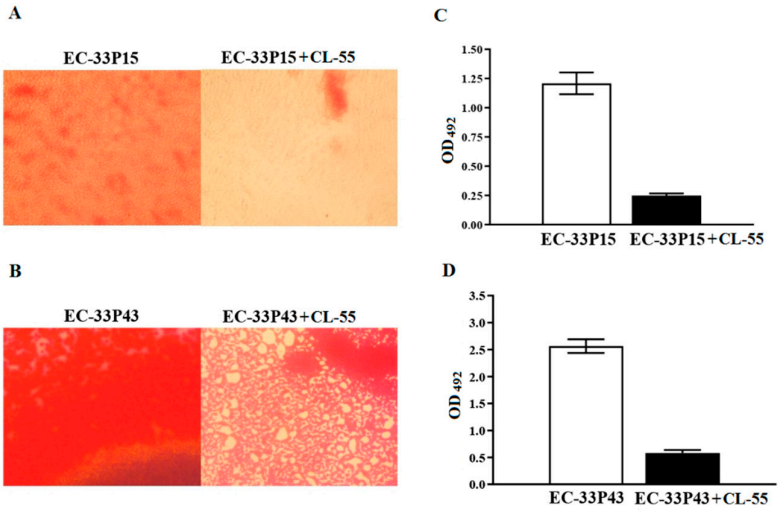

Figure 8. Biofilm formation by *E. coli* isolates in the absence and presence of CL-55 on polystyrene 96-well plates for 72 h. A, B - photomicrograph of crystal violet stained biofilm under light microscopy (200x). C, D - the level of absorbance at 540 nm.

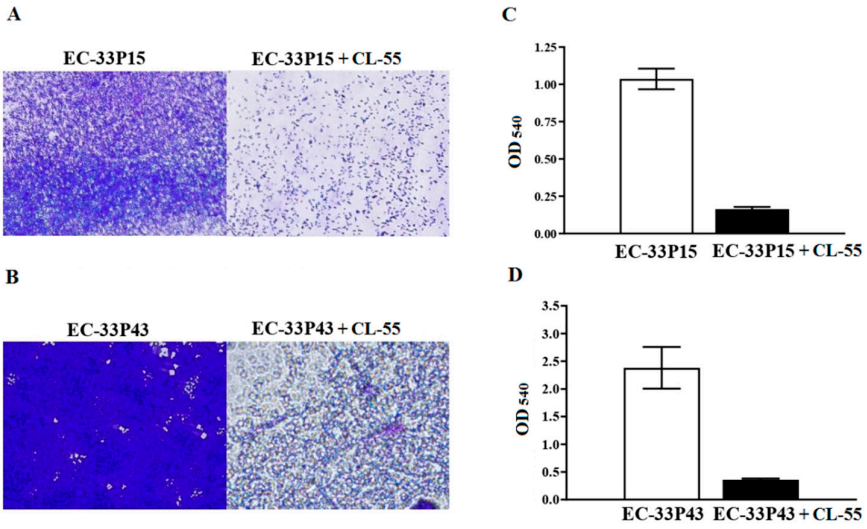

 doi:10.20944/preprints202508.0234.v1

Figure 9. Biofilm formation by *E. coli* isolates in the absence and presence of CL-55 on polystyrene 96-well plates for 72 h. A, B - photomicrograph of Congo red stained biofilm under light microscopy (200x). C, D - the level of absorbance at 492 nm.

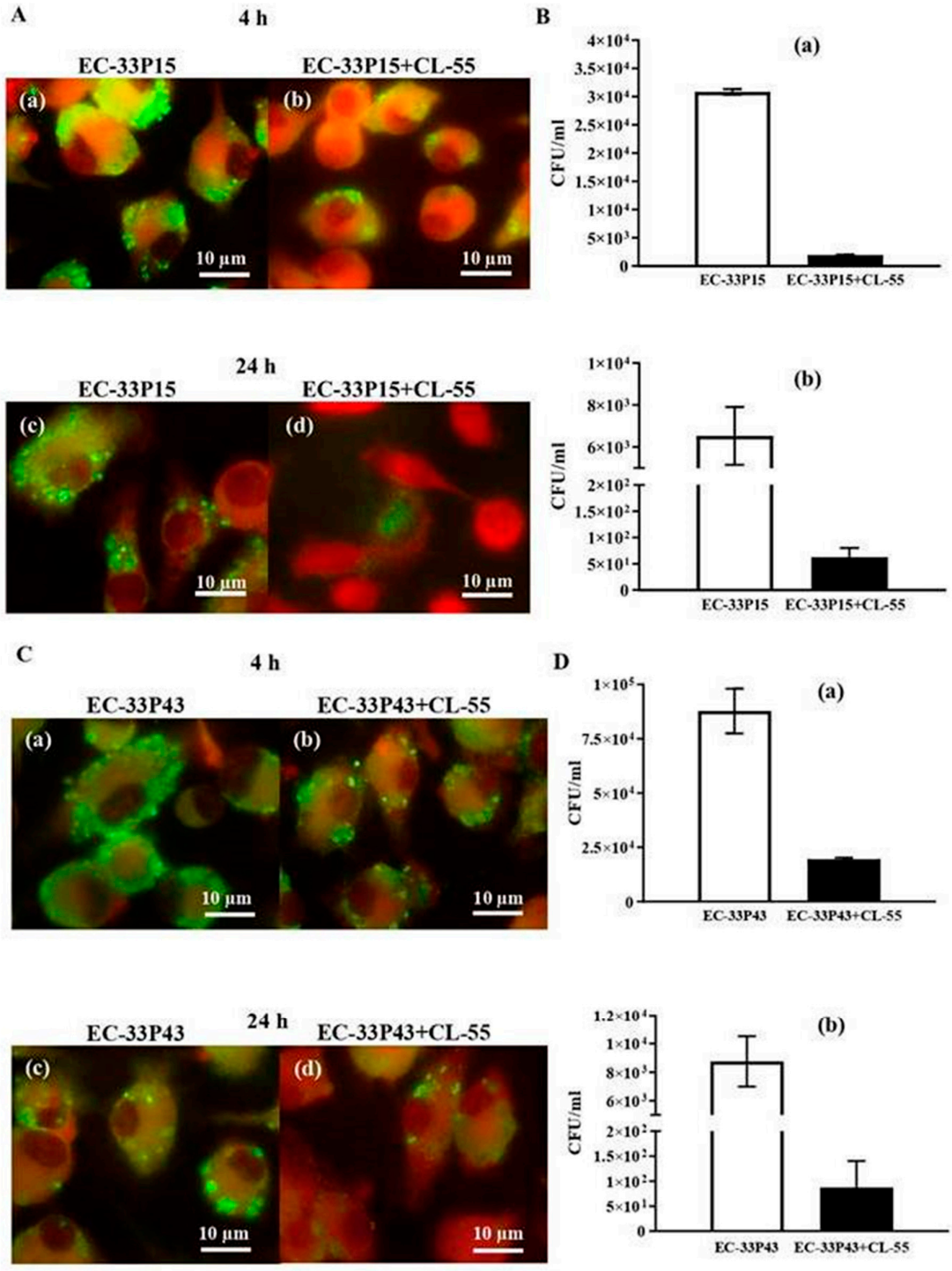

Figure 10. Bacterial survival in RAW264.7 macrophages 4 and 24 h after infection with *E. coli* cultures in the absence and presence of antibacterial drug CL-55. A, C - photomicrographs of the cell culture in the plate at 4 and 24 h of cultivation under a fluorescent microscope (1000×), respectively. A (a, c) and C (a, c) – infected macrophages without CL-55 treatment; A (b, d) and C (b, d) – infected macrophages treated with CL-55. RAW264.7 macrophages are stained with Evans blue (red). Bacteria labeled with indirect FITC-fluorescent antibodies, are green. Scale bar = 10µm.

 doi:10.20944/preprints202508.0234.v1

B, D - bacterial load in macrophages determined by serial plating of macrophage lysates. B (a, b) – CFU of *E. coli* isolate GIMC1402:EC-33P15 after 4 and 24 h; D (a, b) - CFU of *E. coli* isolate GIMC1403:EC-33P43 after 4 and 24 h.

2.3.2. Macrophage Internalization and Survival

Both GIMC1402:EC-33P15 and GIMC1403:EC_33P43 isolates were able to penetrate macrophages. Microscopy of anti-*E. coli* antibody-stained cell monolayer revealed bacterial intracellular communities inside macrophages at 4 and 24 h after interaction of bacteria with macrophages (Figure 10). When macrophages RAW264.7 were infected with GIMC1402:EC-33P15 with MOI 10 ($5x10^6$ CFU/ml), the number of viable intracellular bacteria after 1 h was $3.4×10^4$ CFU/ml, and remained in the same number after 4 h (Figure 10 A (a), B (a)). After 24 h, GIMC1402:EC-33P15 retained the ability to replicate in macrophages and was detected in an amount of $6.5×10^3$ CFU/ml (Figure 10 A (c), B (b)). *E. coli* isolate GIMC1403:EC-33P43 used at MOI 10 formed an order of magnitude greater number of intracellular bacteria ($3.5×10^5$ CFU/ml) at 1 and 4 h after capture by macrophages RAW264.7 (Figure 10 C (a), D (a)). After 24 h of incubation, GIMC1402:EC-33P43 was detected in macrophages in amount of $8.5×10^3$ CFU/ml (Figure 10 C (c), D (b)).

Thus, both CF isolates demonstrated the ability to form biofilms and survive inside macrophages, which explains the long-term chronic respiratory tract infection of patients 119-CF and 149-CF, and the ineffectiveness of antibiotic and CFTR modulator therapy in reducing the bacterial load in the lungs of the patients. Therefore, we tested the sensitivity of CF isolates to the new antibacterial drug Fluorothiazinone (CL-55, the active pharmaceutical ingredient) in biofilms and at intracellular localization.

2.3.3. CL-55 Does not Inhibit Bacterial Viability

The results of a study of the direct antibacterial effect of CL-55 on *E. coli* CF isolates showed that the virulence inhibitor does not inhibit bacterial growth when cultured in vitro at concentrations from 25 to 300 μM.

2.3.4. Effect of the Active Pharmaceutical Ingredient CL-55 on Biofilm Formation and Intracellular Survival of CF Isolates

Returning to Figures 8 and 9, we can see that incubation of CF isolates with CL-55 leads to a decrease in both the amount of biomass and the density of the biofilm, as well as to the suppression of the production of the exopolysaccharide matrix. The biofilm density showed a 6-fold decrease for the GIMC1402:EC-33P15 isolate and a 7-fold decrease for GIMC1403:EC_33P43 (Figure 8 C, D). The production of exopolysaccharide matrix was suppressed by 5 times for the GIMC1402:EC-33P15 isolate and by 4 times for the GIMC1403:EC_33P43 (Figure 9 C, D).

The effect of CL-55 on CF isolates inside macrophages can be seen in Figure 10 (A (b, d), C (b, d)). The introduction of CL-55 simultaneously with *E. coli* GIMC1402:EC-33P15 infection of the RAW264.7 monolayer reduced the bacterial load in macrophages to $2.0×10^3$ CFU/ml and $1.9×10^3$ CFU/ml after 1 and 4 h, respectively (Figure 10 B (a)). After 24 hours, in the presence of CL-55, a significant decrease in viable intracellular bacteria to $6.3×10^1$ CFU/ml was observed (Figure 10 B (b)).

For the *E. coli* isolate GIMC1403:EC-33P43, in the presence of CL-55, the number of intracellular bacteria was decreased by 1 order of magnitude after 1 and 4 hours, and by 2 orders after 24 h (Figure 10 C, D).

Thus, the new antibacterial drug exerted a suppressive effect both on the formation of biofilms by *E. coli* CF isolates and on the proliferation of bacteria inside macrophages.

 doi:10.20944/preprints202508.0234.v1

3. Discussion

Two isolates of *E. coli* ST648 were analyzed in this research. Both strains were from the long-term infected CF patients. The molecular confirmation of the *E. coli* genotype was first made in 2013 and 2015. The time of infection of patients by the CTX-M-15 producing *E. coli* was roughly determined as no earlier than 2006 on the basis of comparison of CF isolates with evolutionary clades of ST648 isolates. These clades were predicted by Schaufler et al. through the Bayesian analysis of the population structure [7].

Whole genome sequencing allowed comparison of chromosomes and episomes of two CF isolates, and confirm the plasticity of the *E. coli* ST648 genomes. As a result of the recombination event, the K5 capsule type in GIMC1402:EC_33P15 is changed to the K4 type in GIMC1403:EC_33P43. Both capsules, heparosan-containing K5 and chrondodontin-containing K4, are associated with the ExPEC [46]. These capsule types mimic polysaccharides present on cells in the human tissues, so they are very poorly immunogenic but very virulent [46,47]. Recombination events also affected the CRISPR region, indicating a different spectrum of bacteriophages with which the isolates could interact. Another result of recombination provided *E. coli* GIMC1402:EC_33P15 with an advantage in utilizing an additional carbon source, propanediol, in a specialized microcompartment.

MGE introduced AMP genes into both the chromosome and plasmid of isolate GIMC1402:EC_33P15, expanding the resistance potential compared to isolate GIMC1403:EC_33P43.

The ESBL genes as markers for *E. coli* ST648 deserve special attention. Both isolates produced ESBL CTX-M-15 and OXA-1, but TEM-1 was a distinctive feature of isolate GIMC1402:EC_33P15. The history of acquisition of ESBL genes by *E. coli* ST648 also shows the genomic plasticity of isolates of this genotype. Let's consider clinical isolates. The first isolate ST648 was registered in the USA in 2007 and produced only ESBL CTX-M-15, as did the isolate of 2008 [48], and the isolate from Tanzania in 2011 [49]. The ESBL spectrum in the 2010 isolates from China [50] and 2015 isolates from Nepal [51] expanded to three: CTX-M-15, OXA-1, and TEM-1, which corresponds to the ESBL set in the GIMC1402:EC_33P15 isolate. In 2011, an isolate from a patient returning to the UK after hospitalization in India produced NDM-5 along with CTX-M-15 and TEM-1 [52]. Finally, in 2023, isolates with CTX-M-15 and KPC-2 were recovered from patients in Argentina [53] and China [54]. The diversity of ESBLs is even greater in isolates from wild birds and farm animals. CTX-M of different alleles: CTX–M–2 [55] or CTX–M–8 [56], or CTX–M–55 [57], can be supplemented with TEM-1 and NDM-5 (*Cairina moschata*) [55] or CMY–2 and AmpC (*Fregata magnificens*) [57]. Thus, MGE facilitates the accumulation of resistance genes by *E. coli* ST648 isolates.

In our study, less resistant in the planktonic state, *E. coli* GIMC1403:EC_33P43 has an advantage in biofilm formation, a protective mechanism that helps to avoid the action of antibiotics. The genome of GIMC1403:EC_33P43 encodes the regulator of biofilm formation BssS, which is probably why isolate GIMC1403:EC_33P43 forms a denser biofilm on the abiotic surface.

The second defense mechanism, survival and reproduction inside eukaryotic cells such as macrophages, worked equally well in two isolates.

Not all antibiotics are effective in killing bacteria inside the eukaryotic cells. The lipophilic compounds are able to passively diffuse through the membrane, so for them the intracellular-to-plasma ratios are greater than 0.5 [58]. The hydrophilic compounds may enter the cells only when in the presence of specific carriers [59]; therefore, the intracellular-to-plasma ratios for them are less than 0.5 [58]. Antibiotics recommended for the treatment of *E. coli* infection belong to the beta-lactam subclasses: cephalosporins and carbapenems, and are hydrophilic compounds. Long-term history of antibacterial treatment of the patients confirms the ineffectiveness of these compounds in the eradication of *E. coli*.

The new antibacterial compound used in our study, Fluorthiazinone (C19H17F2N3O4S) with the active pharmaceutical ingredient CL-55, is lipophilic. The presence of a fluorine atoms enhances the lipophilicity of CL-55 [60]. The lipophilicity ensures rapid drug absorption and transport to tissues, such as spleen, lungs, urinary bladder and prostate, and penetration into eukaryotic cells [61]. The CL-55 doses of 50 μM and 100 μM were not toxic for Mccoy B cells (a hybrid cell line consisting

 doi:10.20944/preprints202508.0234.v1

of human synovial cells and mouse fibroblasts) and peritoneal macrophages, respectively, and were effective in suppressing of the intracellular development of chlamydia and *Salmonella enterica* [60,62]. We used a dose of 47.5 μM to treat the RAW 264.7 macrophages infected with CF isolates of *E. coli*. The residual amount of *E. coli* was 6% of the control after 4 h and 1% after 24 h.

Resistance to lipophilic antibacterial compounds by intracellular bacteria was studied by Garcia-Medina et al. Mouse tracheal epithelial cells infected with a mucoid strain of *Pseudomonas aeruginosa* isolated from a patient with cystic fibrosis were exposed to ciprofloxacin at a concentration of 1.2 mM, which killed planktonic cells [63]. After 24 h of incubation, the number of intracellular bacteria decreased by 16.7 times, i.e. incomplete antibiotic killing was observed [63]. CL-55 at a concentration of 47.5 μM (25 times lower) suppressed intracellular *E. coli* by 103 times after 24 h of incubation.

Biofilms as aggregated microbes surrounded by a self-produced matrix and either adhering to surfaces or located in tissues or secretions [64] are well known in microbiology. However, in medicine, Höiby was the first to propose the concept of biofilm infection and their importance with respect to chronic infections, studying lung infection in cystic fibrosis [65]. Bacteria in biofilm, show increased tolerance to antimicrobials and resist the antimicrobial properties of the host defense [66]. Staudinger et al., using a model system involving gels as growth substrates for *P. aeruginosa*, revealed that aggregates showed 100- to 1,000-fold less killing by tobramycin at a concentration of 21.4 μM as compared with dispersed cells [67]. To study the effect of CL-55 on *E. coli* aggregates, we used a biofilm model on an abiotic surface. CL-55 at a concentration of 238 μM suppressed biofilm formation and exopolysaccharide matrix production by both isolates, GIMC1402:EC_33P15 and GIMC1403:EC_33P43, despite the denser biofilm of the latter. Thus, CL-55 was effective against the two most resistant states of bacteria in lung infections: intracellular and aggregate. Since Fluorothiazinon is recommended as an adjunctive therapy, the main antibacterial drug will have to cope with the less resistant planktonic form of infection.

4. Materials and Methods

4.1. Materials

Sputum samples were obtained from two CF patients, 119-CF and 149-CF, with severe lung disease who were in a clinical state without exacerbation and receiving maintenance therapy. Patient 149-CF had also been taking a dual CFTR modulator therapy Lumacaftor / Ivacaftor for 2.2 years.

Antibacterial drug Fluorthiazinone (C19H17F2N3O4S; FT) and its active pharmaceutical ingredient CL-55 [25] was used for in vitro experiments. A stock CL-55 solution for biofilm assay was 4.8 mM in 0,1 M sodium acetate pH 7.0 ± 0.2. When working with cell lines, a stock CL-55 solution 26,1 mM in dimethyl sulfoxide (DMSO) was used.

4.2. Methods

Bacteria isolation and cultivation

E. coli was isolated on 5% blood agar and Endo agar. The isolates GIMC1402:EC_33P15 and GIMC1403:EC_33P43 were cultured in Luria-Bertani (LB) broth at 37°C.

Isolate identification

To identify the isolates, two targets were amplified: *16S rDNA* with primers [68] and *adk* with primers adkF-12 (in home elaborated) and adkR1 [69], then amplicons were sequenced as described in [70], and identified by BLAST NCBI and the *Escherichia* typing database (https://pubmlst.org/bigsdb?db=pubmlst_escherichia_seqdef).

Microbiome analysis

The sputum microbiome composition was determined by massively parallel sequencing of the *16S rDNA* gene amplicons with the Illumina platform. The results, deposited in GenBank (bioproject PRJNA717158), were analyzed by the Microbial Genomics Module of the CLC Genomic Workbench v.21.0.1 package (QIAGEN, USA), Greengenes v13_8 database with a similarity level of 97% was used

 doi:10.20944/preprints202508.0234.v1

for determination of Operational Taxonomic Units (OTU). The Shannon entropy index and the coefficient of phylogenetic diversity (PD) were used to assess alpha diversity.

Whole genome sequencing.

The genomes of the strains GIMC1402:EC_33P15 and GIMC1403:EC_33P43 were sequenced on the Illumina platform. The NadPrep EZ DNA Library Preparation protocol (Nanodigmbio (Nanjing) Biotechnology Co. Ltd., Nanjing, Jiangsu, China) and the KAPA HyperPlus Kit (F. Hoffmann-La Roche Ltd, Switzerland) protocol were used for the library's preparation. Sequencing was performed on MiSeq and NextSeq 500/550 (Illumina, San Diego, CA, USA). Genomes were assembled using CLC Genomics Workbench v. 21 (QIAGEN) and SPAdes v. 3.13.0 (St. Petersburg genome assembler, Russia, URL: http://cab.spbu.ru/software/spades/, accessed on 05 May 2025) [71]. The software Rapid Annotations Subsystems Technology (RAST) and SEED [72] and the NCBI Prokaryotic Genome Annotation Pipeline (PGAP) [73] were used for genome annotation. WGS data are available in GenBank: BioProject PRJNA561493, Accession Numbers: CP181181-CP181185 and CP181392-CP181397.

Genome analysis

For virulence factor identification, the VFDB (virulence factor database, http://www.mgc.ac.cn/VFs/, accessed on 05 May 2025) database [74], Pathogenwatch v21.0.0 (https://pathogen.watch/, accessed on 05 May 2025), and BlastKOALA (KEGG Orthology And Links Annotation, https://www.kegg.jp/blastkoala/, accessed on 05 May 2025) [75] were used. The spectrums of antimicrobial resistance genes were determined using the CARD (Comprehensive Antibiotic Resistance Database, https://card.mcmaster.ca/, accessed on 05 May 2025) resource [76] and BV-BRC (Bacterial and Viral Bioinformatics Resource Center, https://www.bv-brc.org/, accessed on 05 May 2025), formed on the basis of PATRIC [77]. To clarify the annotation of beta-lactamases, the Beta-lactamase database (BLDB, http://bldb.eu/, accessed on 05 May 2025) [78] was consulted.

The search for mobile elements and associated genes was performed using ISAbR-0.1.6 [79] and MGE MobileElementFinder v1.0.3 (https://cge.food.dtu.dk/services/MobileElementFinder/, accessed on 05 May 2025) [80]. PlasmidFinder 2.1 (https://cge.food.dtu.dk/services/PlasmidFinder/, accessed on 05 May 2025) [81] was applied to identify incompatibility groups (Incompatibility, Inc) of plasmid replicons. For rapid identification, annotation, and visualization of prophage sequences in bacterial genomes and plasmids, the PHASTEST web server (PHAge Search Tool with Enhanced Sequence Translation https://phastest.ca/, accessed on 05 May 2025) was used [82]. The CRISPRCasFinder program (https://crisprcas.i2bc.paris-saclay.fr/CrisprCasFinder/Index, accessed on 05 May 2025) [83] was applied for detection of CRISPRs and cas genes.

To compare the nucleotide sequences and proteomes, the off-line BLAST-2.10.0+ program (https://ftp.ncbi.nlm.nih.gov/blast/executables/blast+/LATEST/) was used. Visualization of the results of comparative chromosome analysis was performed using the BRIG 0.95 program (BLAST Ring Image Generator, http://sourceforge.net/projects/brig/, accessed on 05 May 2025) [84]. Comparison of plasmid sequences was visualized by the Artemis Comparison Tool (Sanger, Cambridge, UK) [85].

The Create Average Nucleotide Identity Comparison tool of CLC Genomics Workbench (QIAGEN, Germantown, MD, USA) was used to calculate two measures: the Alignment Percentage (AP) and the Average Nucleotide Identity (ANI).

Phylogenetic analysis.

Preliminary determination of the phylogenetic group affiliation of the analyzed isolates was performed based on the scheme proposed by Clermont O. et al. [86]. The analysis was done in silico, and the corresponding gene fragments from the reference genomes: TspE4.C2 and *aceK* (CP161809.1), *chuA* (U67920.1), and *yjaA* (NC_000913.3) were compared using the BLAST-2.10.0+ program with the sequences of the complete genomes of the strains GIMC1402:EC_33P15 and GIMC1403:EC_33P43.

More complicated analysis included the alignment of concatenated nucleotide sequences of the MLST scheme of Achtman and Pasteur (except for the *uidA* gene) and the *aceK* gene fragment from

 doi:10.20944/preprints202508.0234.v1

the scheme proposed by Clermont O. et al. [86], and phylogenetic tree conduction in the MEGA11 program [86]. *E. coli* genomes of different phylogenetic groups A (NZ_CP033020, AP009048.1), B1 (NC_011748.1, CP101307.1), B2 (NZ_MIPU00000000, NZ_CP051263), C (NZ_NXOC00000000, NZ_NKDU00000000), D (NC_011751.1, ADBA00000000), E (NC_002695.2, AEXG00000000.1), and F (NC_011750.1, AEXF00000000.1) were applied as references. For the phylogenetic tree rooting the type strain of *E. fergusonii* ATCC 35469 (NC_011740.1) was used as an outgroup.

Evaluation of the antibacterial effect of CL-55

50 μl of the overnight culture of *E. coli* isolates was added to test tubes with 5 ml of LB broth containing different concentrations of CL-55: 0, 25, 50, 100, 200, 300 μM and cultured in a shaker incubator at 37ºC and 250 rpm for 20 h. The number of viable bacteria was determined by serial dilutions and seeding on LB agar. The results were taken into account after 24 hours of cultivation at 37°C.

Biofilm assay

96-well polystyrene plates were used for static biofilm formation on abiotic surface. Overnight culture of *E. coli* isolates was adjusted to OD600 = 0.5. Evaluation of the effectiveness of CL-55 on biofilm formation was carried out using concentrations of 238 μM. CL-55 was added simultaneously with culture *E. coli* GIMC1402:EC-33P15 and GIMC1403:EC-33P43. LB broth was used as a negative control, and the *E. coli* culture without CL-55 was used as a positive control. The plates were incubated at 37°C for 72 h. Further, the wells were washed with phosphate-buffered saline (PBS) to remove the non-adherent cells. For biomass quantification, biofilm was stained with 0,1% Crystal Violet (CV) solution for 15 min. For extracellular matrix quantification, 0.1% Congo red (CR) was added to the wells and incubated for 30 min. In order to remove excess dye, the wells were rinsed three times with sterile distilled water. For quantitative analysis, dye bound to the biofilm was dissolved in 96% ethanol. The wells were read in a Multiskan EX microplate absorbance reader for CV and CR dyes at wavelengths of 540 and 492 nm, respectively. For visual analysis, plates with fixed, CV- and CR-stained biofilms were examined under a Nikon Eclipse 50i light microscope (Nikon, Japan) at a magnification of 20×. Each *E. coli* isolate was tested in 3 replicates per experiment and in at least three experiments.

Macrophage cell culture and growth conditions

RAW 264.7, which is a macrophage cell line that was established from a tumor in a male mouse induced with the Abelson murine leukemia virus, was used. RAW264.7 cells were incubated in RPMI-1640 cell medium supplemented with 5% FBS without the addition of antibiotics at 37°C with 5% CO_2 for 24 h. After, cell counts were measured.

Bacterial intracellular survival in RAW264.7 macrophages.

For infection of RAW264.7 macrophages, 24-well glass plates (d=12 mm) were used. Macrophages were infected with *E. coli* isolates with an MOI of 10 relative to macrophage cells of 1.3×10^5 cells/ml. To evaluate the effect of CL-55 on the ability of the isolates of *E. coli* to penetrate and survive within macrophages, CL-55 was added to the wells at a final concentration of 47.5 μM simultaneously with infection. Incubation was carried out for 3 h at 37° C and 5% CO_2. Then, the plates were washed, gentamicin at a concentration of 100 μg/ml was added to the wells, and incubated for 1 h to get rid of plankton cells. The plates were then washed to remove plankton and gentamicin contained in the medium. Uninfected RAW264.7 cells were used as a negative control. Infected cells incubated without the addition of CL-55 served as a positive control. The results were then evaluated microscopically and by seeding on LB agar for 24 h. For microscopic analysis, slides were fixed with methanol, incubated with mouse antibodies to *E. coli* for 30 min at 37° C and 5% CO_2, and stained with anti-mouse IgG-FITC conjugate (Merck, New Jersey, USA) for 30 min at 37° C and 5% CO_2. The study was performed under a fluorescence microscope Nikon Eclipse 50i (Nikon, Japan) at 1000× magnification under oil immersion. For quantitative characterization, infected macrophages with and without the addition of CL-55 were lysed with 0.25% Triton X-100 (Sigma, USA). The lysates

 doi:10.20944/preprints202508.0234.v1

were then cultured on LB agar by serial dilutions. All quantitative analyses were performed in triplicate.

To evaluate the effect of CL-55 on the ability of the isolates of *E. coli* to survive and multiplicate within macrophages, CL-55 was added to the wells at a final concentration of 47.5 μM simultaneously with infection and 4 h later. Incubation was carried out for 24 h. One hour before the end of incubation, the plates were washed and gentamicin was added to eliminate plankton. The plates were then washed to remove plankton and gentamicin contained in the medium. Uninfected RAW264.7 cells were used as a negative control. Infected cells incubated without the addition of CL-55 served as a positive control. The results were then evaluated as described earlier.

5. Conclusions

The study of two hypermucoviscous *E. coli* isolates, representatives of the globally distributed clone ST648, demonstrated their high adaptability to long-term persistence. Invasiveness, biofilm formation, survival and proliferation inside eukaryotic cells provide high resistance to the host immune system and recommended antibiotic therapy. Even the addition of CFTR modulators for more than 2 years did not ensure eradication of *E. coli* in patient 149-CF. The efficacy of Fluorothiazinone (CL-55) against CF isolates, both in aggregates and inside macrophages, demonstrated in in vitro experiments, suggests that the use of Fluorothiazinone as a combinative therapy will facilitate eradication of pathogenic microorganisms in the respiratory tract of patients with cystic fibrosis.

6. Patents

Sputum samples from two adult patients were included in the study. The age of patient 119-CF was 39 years, and that of patient 149-CF was 29 years. The duration of infection with *E. coli* ST648, confirmed by molecular genetic methods, was 10 years for patient 119-CF and 9 years for patient 149-CF at the time of isolation of the described strains of *E. coli* ST648.

Author Contributions: Conceptualization, O.L.V., N.A.Z.; methodology, O.L.V., N.N.R., M.S.K., E.I.E., E.L.A., N.A.Z.; software, N.N.R., M.S.K., and E.I.E.; validation, O.L.V., N.N.R., M.S.K., and E.I.E.; formal analysis, N.N.R., M.S.K., E.I.E., E.R.G.; investigation, O.L.V., N.N.R., M.S.K., E.I.E., E.R.G., E.A.K., L.N.K., and E.Y.M.; resources, O.L.V., N.A.Z., and E.L.A.; data curation, M.S.K., N.N.R., O.L.V., and N.A.Z.; writing—original draft preparation, O.L.V., N.N.R., M.S.K., E.I.E., E.R.G., E.A.K.; writing—review and editing, O.L.V., N.A.Z., N.N.R., M.S.K. and E.I.E..; visualization, M.S.K., N.N.R., O.L.V., E.A.K.; supervision, O.L.V., N.A.Z.; project administration, O.L.V., N.A.Z; funding acquisition, O.L.V., N.A.Z. All authors have read and agreed to the published version of the manuscript.

Funding: The study is supported by the State assignment of the N.F. Gamaleya National Research Center for Epidemiology and Microbiology (No. 056-00066-23-00)

Institutional Review Board Statement: The research protocol was approved by the Biomedical Ethics Committee of the N.F. Gamaleya National Research Center for Epidemiology and Microbiology (protocol No. 59, September 8, 2023), and by the Ethics Committee of the Research Institute of Pulmonology under FMBA of Russia (protocol No. 04-23, April 24, 2023 and protocol No. 07-24, December 18, 2024).

Informed Consent Statement: The study was carried out with the informed consent of the patients.

Data Availability Statement: The reported results can be found in the GenBank. Accession Numbers: CP181181-CP181185, CP181392-CP181397, and bioproject PRJNA717158.

Acknowledgments: The authors are grateful to the microbiologist Burmistrov E.M. for isolation *E. coli* and for providing isolates for the study.

Conflicts of Interest: The authors declare no conflicts of interest.

 doi:10.20944/preprints202508.0234.v1

Abbreviations

The following abbreviations are used in this manuscript:

ExPEC	Extraintestinal pathogenic *E. coli*
CAP	Community-acquired pneumonia
NP	Nosocomial pneumonia
VAP	Ventilator-associated pneumonia
CF	Cystic Fibrosis
CPS	Capsular polysaccharide
FT	Fluorthiazinone
CL-55	The active pharmaceutical ingredient of Fluorthiazinone
T3SS	Type 3 secretion system
T6SS	Type 6 secretion system
P-P	Phage-plasmid
ORF	Open reading frame
TRAP	Tripartite ATP-independent periplasmic transporter
ECF	energy-coupling factor
CRISPR	Clustered Regularly Interspaced Short Palindromic Repeats
ESBL	Extended-spectrum beta-lactamase
CA	Colanic acid
ETT2	E. coli type 3 secretion system 2

References

1. Marrie TJ, Fine MJ, Obrosky DS, Coley C, Singer DE, Kapoor WN. Community-acquired pneumonia due to Escherichia coli. Clin Microbiol Infect. 1998;4(12):717-723. doi: 10.1111/j.1469-0691.1998.tb00657.x.
2. La Combe B, Clermont O, Messika J, Eveillard M, Kouatchet A, Lasocki S, Corvec S, Lakhal K, Billard-Pomares T, Fernandes R, Armand-Lefevre L, Bourdon S, Reignier J, Fihman V, de Prost N, Bador J, Goret J, Wallet F, Denamur E, Ricard JD; COLOCOLI group; COLOCOLI Group. Pneumonia-Specific Escherichia coli with Distinct Phylogenetic and Virulence Profiles, France, 2012-2014. Emerg Infect Dis. 2019;25(4):710-718. doi: 10.3201/eid2504.180944.
3. John TM, Deshpande A, Brizendine K, Yu PC, Rothberg MB. Epidemiology and Outcomes of Community-Acquired Escherichia coli Pneumonia. Open Forum Infect Dis. 2021;9(1):ofab597. doi: 10.1093/ofid/ofab597.
4. Messika J, Magdoud F, Clermont O, Margetis D, Gaudry S, Roux D, Branger C, Dreyfuss D, Denamur E, Ricard JD. Pathophysiology of Escherichia coli ventilator-associated pneumonia: implication of highly virulent extraintestinal pathogenic strains. Intensive Care Med. 2012;38(12):2007-2016. doi: 10.1007/s00134-012-2699-5.
5. Koulenti D, Tsigou E, Rello J. Nosocomial pneumonia in 27 ICUs in Europe: perspectives from the EU-VAP/CAP study. Eur J Clin Microbiol Infect Dis. 2017;36(11):1999-2006. doi: 10.1007/s10096-016-2703-z.
6. Stoesser N, Sheppard AE, Pankhurst L, De Maio N, Moore CE, Sebra R, Turner P, Anson LW, Kasarskis A, Batty EM, Kos V, Wilson DJ, Phetsouvanh R, Wyllie D, Sokurenko E, Manges AR, Johnson TJ, Price LB, Peto TE, Johnson JR, Didelot X, Walker AS, Crook DW; Modernizing Medical Microbiology Informatics Group (MMMIG). Evolutionary History of the Global Emergence of the Escherichia coli Epidemic Clone ST131. mBio. 2016 Mar 22;7(2):e02162. doi: 10.1128/mBio.02162-15.
7. Schaufler K, Semmler T, Wieler LH, Trott DJ, Pitout J, Peirano G, Bonnedahl J, Dolejska M, Literak I, Fuchs S, Ahmed N, Grobbel M, Torres C, McNally A, Pickard D, Ewers C, Croucher NJ, Corander J, Guenther S. Genomic and Functional Analysis of Emerging Virulent and Multidrug-Resistant Escherichia coli Lineage Sequence Type 648. Antimicrob Agents Chemother. 2019;63(6):e00243-19. doi: 10.1128/AAC.00243-19.
8. GBD 2021 Antimicrobial Resistance Collaborators. Global burden of bacterial antimicrobial resistance 1990-2021: a systematic analysis with forecasts to 2050. Lancet. 2024;404(10459):1199-1226. doi: 10.1016/S0140-6736(24)01867-1.
9. Zemanick ET, Hoffman LR. Cystic Fibrosis: Microbiology and Host Response. Pediatr Clin North Am. 2016;63(4):617-36. doi: 10.1016/j.pcl.2016.04.003.

 doi:10.20944/preprints202508.0234.v1

10. Barillova P, Tchesnokova V, Dübbers A, Küster P, Peters G, Dobrindt U, Sokurenko EV, Kahl BC. Prevalence and persistence of Escherichia coli in the airways of cystic fibrosis patients - an unrecognized CF pathogen? Int J Med Microbiol. 2014;304(3-4):415-21. doi: 10.1016/j.ijmm.2014.02.008.
11. Edwards BD, Somayaji R, Greysson-Wong J, Izydorczyk C, Waddell B, Storey DG, Rabin HR, Surette MG, Parkins MD. Clinical Outcomes Associated With Escherichia coli Infections in Adults With Cystic Fibrosis: A Cohort Study. Open Forum Infect Dis. 2019;7(1):ofz476. doi: 10.1093/ofid/ofz476.
12. Izydorczyk C, Waddell B, Edwards BD, Greysson-Wong J, Surette MG, Somayaji R, Rabin HR, Conly JM, Church DL, Parkins MD. Epidemiology of E. coli in Cystic Fibrosis Airways Demonstrates the Capacity for Persistent Infection but Not Patient-Patient Transmission. Front Microbiol. 2020;11:475. doi: 10.3389/fmicb.2020.00475.
13. Registry of patients with cystic fibrosis in the Russian Federation. 2023. Editors Amelina E.L., Kashirskaya N.Yu., Kondratyeva E.I., et al.; Publishing House "MEDPRACTIKA-M", Moscow, Russia, 2025.
14. Whitfield C. Biosynthesis and assembly of capsular polysaccharides in Escherichia coli. Annu Rev Biochem. 2006;75:39-68. doi: 10.1146/annurev.biochem.75.103004.142545.
15. Xue P, Corbett D, Goldrick M, Naylor C, Roberts IS. Regulation of expression of the region 3 promoter of the Escherichia coli K5 capsule gene cluster involves H-NS, SlyA, and a large 5' untranslated region. J Bacteriol. 2009;191(6):1838-46. doi: 10.1128/JB.01388-08.
16. Harris S, Piotrowska MJ, Goldstone RJ, Qi R, Foster G, Dobrindt U, Madec JY, Valat C, Rao FV, Smith DGE. Variant O89 O-Antigen of *E. coli* Is Associated With Group 1 Capsule Loci and Multidrug Resistance. Front Microbiol. 2018;9:2026. doi: 10.3389/fmicb.2018.02026.
17. Cheng HY, Chen YS, Wu CY, Chang HY, Lai YC, Peng HL. RmpA regulation of capsular polysaccharide biosynthesis in Klebsiella pneumoniae CG43. J Bacteriol. 2010;192(12):3144-58. doi: 10.1128/JB.00031-10.
18. Neumann B, Lippmann N, Wendt S, Karlas T, Lübbert C, Werner G, Pfeifer Y, Schuster CF. Recurrent bacteremia with a hypermucoviscous Escherichia coli isolated from a patient with perihilar cholangiocarcinoma: insights from a comprehensive genome-based analysis. Ann Clin Microbiol Antimicrob. 2022;21(1):28. doi: 10.1186/s12941-022-00521-7.
19. Lin YT, Jeng YY, Chen TL, Fung CP. Bacteremic community-acquired pneumonia due to Klebsiella pneumoniae: clinical and microbiological characteristics in Taiwan, 2001-2008. BMC Infect Dis. 2010;10:307. doi: 10.1186/1471-2334-10-307.
20. Han B, Li M, Xu Y, Islam D, Khang J, Del Sorbo L, Lee W, Szaszi K, Zhong N, Slutsky AS, Li Y, Zhang H. Tsr Chemoreceptor Interacts With IL-8 Provoking E. coli Transmigration Across Human Lung Epithelial Cells. Sci Rep. 2016;6:31087. doi: 10.1038/srep31087.
21. Grubwieser P, Hoffmann A, Hilbe R, Seifert M, Sonnweber T, Böck N, Theurl I, Weiss G, Nairz M. Airway Epithelial Cells Differentially Adapt Their Iron Metabolism to Infection With Klebsiella pneumoniae and Escherichia coli In Vitro. Front Cell Infect Microbiol. 2022;12:875543. doi: 10.3389/fcimb.2022.875543.
22. Zhuge X, Sun Y, Jiang M, Wang J, Tang F, Xue F, Ren J, Zhu W, Dai J. Acetate metabolic requirement of avian pathogenic Escherichia coli promotes its intracellular proliferation within macrophage. Vet Res. 2019;50(1):31. doi: 10.1186/s13567-019-0650-2.
23. Zhuge X, Sun Y, Xue F, Tang F, Ren J, Li D, Wang J, Jiang M, Dai J. A Novel PhoP/PhoQ Regulation Pathway Modulates the Survival of Extraintestinal Pathogenic Escherichia coli in Macrophages. Front Immunol. 2018;9:788. doi: 10.3389/fimmu.2018.00788.
24. Nazareth H, Genagon SA, Russo TA. Extraintestinal pathogenic Escherichia coli survives within neutrophils. Infect Immun. 2007;75(6):2776-85. doi: 10.1128/IAI.01095-06.
25. Zigangirova NA, Lubenec NL, Beloborodov VB, Sheremet AB, Nelyubina SA, Bondareva NE, Zakharov KA, Luyksaar SI, Zolotov SA, Levchenko EU, Luyksaar SV, Koroleva EA, Fedina ED, Simakova YV, Pushkar DY, Gintzburg AL. A New "Non-Traditional" Antibacterial Drug Fluorothiazinone-Clinical Research in Patients with Complicated Urinary Tract Infections. Antibiotics (Basel). 2024;13(6):476. doi: 10.3390/antibiotics13060476.
26. Pfeifer E, Moura de Sousa JA, Touchon M, Rocha EPC. Bacteria have numerous distinctive groups of phage-plasmids with conserved phage and variable plasmid gene repertoires. Nucleic Acids Res. 2021;49(5):2655-2673. doi: 10.1093/nar/gkab064.

 doi:10.20944/preprints202508.0234.v1

27. Boyd JM, Sondelski JL, Downs DM. Bacterial ApbC protein has two biochemical activities that are required for in vivo function. J Biol Chem. 2009;284(1):110-118. doi: 10.1074/jbc.M807003200.
28. Jurėnas D, Fraikin N, Goormaghtigh F, Van Melderen L. Biology and evolution of bacterial toxin-antitoxin systems. Nat Rev Microbiol. 2022;20(6):335-350. doi: 10.1038/s41579-021-00661-1.
29. Akhtar AA, Turner DP. The role of bacterial ATP-binding cassette (ABC) transporters in pathogenesis and virulence: Therapeutic and vaccine potential. Microb Pathog. 2022;171:105734. doi: 10.1016/j.micpath.2022.105734.
30. Sabri M.; Léveillé S.; Dozois CM. A SitABCD homologue from an avian pathogenic Escherichia coli strain mediates transport of iron and manganese and resistance to hydrogen peroxide. Microbiology 2006, 152(Pt 3):745-758.
31. Hrovat K.; Zupančič JČ.; Seme K, Avguštin JA. QAC Resistance Genes in ESBL-Producing E. coli Isolated from Patients with Lower Respiratory Tract Infections in the Central Slovenia Region—A 21-Year Survey. Trop Med Infect Dis 2023, 8(5):273.
32. Virolle C, Goldlust K, Djermoun S, Bigot S, Lesterlin C. Plasmid Transfer by Conjugation in Gram-Negative Bacteria: From the Cellular to the Community Level. Genes (Basel). 2020;11(11):1239. doi: 10.3390/genes11111239.
33. Ghigo JM. Natural conjugative plasmids induce bacterial biofilm development. Nature. 2001;412(6845):442-5. doi: 10.1038/35086581.
34. Barrios AF, Zuo R, Ren D, Wood TK. Hha, YbaJ, and OmpA regulate Escherichia coli K12 biofilm formation and conjugation plasmids abolish motility. Biotechnol Bioeng. 2006;93(1):188-200. doi: 10.1002/bit.20681.
35. Okshevsky M, Meyer RL. The role of extracellular DNA in the establishment, maintenance and perpetuation of bacterial biofilms. Crit Rev Microbiol. 2015;41(3):341-52. doi: 10.3109/1040841X.2013.841639.
36. Jurėnas D.; Fraikin N.; Goormaghtigh F.; Van Melderen L. Biology and evolution of bacterial toxin-antitoxin systems. Nat Rev Microbiol. 2022, 20(6):335-350.
37. Boos W. Binding protein-dependent ABC transport system for glycerol 3-phosphate of Escherichia coli. Methods Enzymol. 1998;292:40-51. doi: 10.1016/s0076-6879(98)92006-7.
38. Karimova G, Davi M, Ladant D. The β-lactam resistance protein Blr, a small membrane polypeptide, is a component of the Escherichia coli cell division machinery. J Bacteriol. 2012;194(20):5576-88. doi: 10.1128/JB.00774-12.
39. Wong RS, McMurry LM, Levy SB. 'Intergenic' blr gene in Escherichia coli encodes a 41-residue membrane protein affecting intrinsic susceptibility to certain inhibitors of peptidoglycan synthesis. Mol Microbiol. 2000;37(2):364-70. doi: 10.1046/j.1365-2958.2000.01998.x.
40. Davies JS, Currie MJ, North RA, Scalise M, Wright JD, Copping JM, Remus DM, Gulati A, Morado DR, Jamieson SA, Newton-Vesty MC, Abeysekera GS, Ramaswamy S, Friemann R, Wakatsuki S, Allison JR, Indiveri C, Drew D, Mace PD, Dobson RCJ. Structure and mechanism of a tripartite ATP-independent periplasmic TRAP transporter. Nat Commun. 2023;14(1):1120. doi: 10.1038/s41467-023-36590-1.
41. Domka J, Lee J, Wood TK. YliH (BssR) and YceP (BssS) regulate Escherichia coli K-12 biofilm formation by influencing cell signaling. Appl Environ Microbiol. 2006;72(4):2449-59. doi: 10.1128/AEM.72.4.2449-2459.2006.
42. Guiral E, Mendez-Arancibia E, Soto SM, Salvador P, Fabrega A, Gascon J, Vila J. CTX-M-15-producing enteroaggregative Escherichia coli as cause of travelers' diarrhea. Emerg Infect Dis. 2011 Oct;17(10):1950-3. doi: 10.3201/eid1710.110022.
43. Chen J, Lee SM, Mao Y. Protective effect of exopolysaccharide colanic acid of Escherichia coli O157:H7 to osmotic and oxidative stress. Int J Food Microbiol. 2004;93(3):281-6. doi: 10.1016/j.ijfoodmicro.2003.12.004.
44. Hayashi T, Makino K, Ohnishi M, Kurokawa K, Ishii K, Yokoyama K, Han CG, Ohtsubo E, Nakayama K, Murata T, Tanaka M, Tobe T, Iida T, Takami H, Honda T, Sasakawa C, Ogasawara N, Yasunaga T, Kuhara S, Shiba T, Hattori M, Shinagawa H. Complete genome sequence of enterohemorrhagic Escherichia coli O157:H7 and genomic comparison with a laboratory strain K-12. DNA Res. 2001;8(1):11-22. doi: 10.1093/dnares/8.1.11.

 doi:10.20944/preprints202508.0234.v1

45. Cui Z, Yang CH, Kharadi RR, Yuan X, Sundin GW, Triplett LR, Wang J, Zeng Q. Cell-length heterogeneity: a population-level solution to growth/virulence trade-offs in the plant pathogen Dickeya dadantii. PLoS Pathog. 2019;15(8):e1007703. doi: 10.1371/journal.ppat.1007703.
46. Arredondo-Alonso S, Blundell-Hunter G, Fu Z, Gladstone RA, Fillol-Salom A, Loraine J, Cloutman-Green E, Johnsen PJ, Samuelsen Ø, Pöntinen AK, Cléon F, Chavez-Bueno S, De la Cruz MA, Ares MA, Vongsouvath M, Chmielarczyk A, Horner C, Klein N, McNally A, Reis JN, Penadés JR, Thomson NR, Corander J, Taylor PW, McCarthy AJ. Evolutionary and functional history of the Escherichia coli K1 capsule. Nat Commun. 2023 Jun 15;14(1):3294. doi: 10.1038/s41467-023-39052-w.
47. Rodriguez ML, Jann B, Jann K. Structure and serological characteristics of the capsular K4 antigen of Escherichia coli O5:K4:H4, a fructose-containing polysaccharide with a chondroitin backbone. Eur J Biochem. 1988 Oct 15;177(1):117-24. doi: 10.1111/j.1432-1033.1988.tb14351.x.
48. Sidjabat HE, Paterson DL, Adams-Haduch JM, Ewan L, Pasculle AW, Muto CA, Tian GB, Doi Y. Molecular epidemiology of CTX-M-producing Escherichia coli isolates at a tertiary medical center in western Pennsylvania. Antimicrob Agents Chemother. 2009;53(11):4733-9. doi: 10.1128/AAC.00533-09.
49. Mshana SE, Imirzalioglu C, Hain T, Domann E, Lyamuya EF, Chakraborty T. Multiple ST clonal complexes, with a predominance of ST131, of Escherichia coli harbouring blaCTX-M-15 in a tertiary hospital in Tanzania. Clin Microbiol Infect. 2011;17(8):1279-82. doi: 10.1111/j.1469-0691.2011.03518.x.
50. Zong Z, Yu R. Escherichia coli carrying the blaCTX-M-15 gene of ST648. J Med Microbiol. 2010;59(Pt 12):1536-1537. doi: 10.1099/jmm.0.022459-0.
51. Sherchan JB, Hayakawa K, Miyoshi-Akiyama T, Ohmagari N, Kirikae T, Nagamatsu M, Tojo M, Ohara H, Sherchand JB, Tandukar S. Clinical epidemiology and molecular analysis of extended-spectrum-β-lactamase-producing Escherichia coli in Nepal: characteristics of sequence types 131 and 648. Antimicrob Agents Chemother. 2015;59(6):3424-32. doi: 10.1128/AAC.00270-15.
52. Ewers C, Bethe A, Semmler T, Guenther S, Wieler LH. Extended-spectrum β-lactamase-producing and AmpC-producing Escherichia coli from livestock and companion animals, and their putative impact on public health: a global perspective. Clin Microbiol Infect. 2012;18(7):646-55. doi: 10.1111/j.1469-0691.2012.03850.x.
53. Piekar M, Álvarez VE, Knecht C, Leguina C, García Allende N, Carrera Páez L, Gambino AS, González Machuca A, Campos J, Fox B, Carpio E, Aguilar A, Alonso FM, Fernández Canigia L, Quiroga MP, Centrón D. Genomic data reveals the emergence of the co-occurrence of blaKPC-2 and blaCTX-M-15 in an Escherichia coli ST648 strain isolated from rectal swab within the framework of hospital surveillance. J Glob Antimicrob Resist. 2023;32:108-112. doi: 10.1016/j.jgar.2022.12.012.
54. He X, Xu L, Dai H, Ge M, Zhu J, Fu H, Zhu S, Shao J. Genomic Characteristics of a Multidrug-Resistant ST648 Escherichia coli Isolate Co-Carrying blaKPC-2 and blaCTX-M-15 Genes Recovered from a Respiratory Infection in China. Infect Drug Resist. 2023;16:3535-3540. doi: 10.2147/IDR.S415846.
55. Yang RS, Feng Y, Lv XY, Duan JH, Chen J, Fang LX, Xia J, Liao XP, Sun J, Liu YH. Emergence of NDM-5- and MCR-1-Producing Escherichia coli Clones ST648 and ST156 from a Single Muscovy Duck (Cairina moschata). Antimicrob Agents Chemother. 2016;60(11):6899-6902. doi: 10.1128/AAC.01365-16.
56. Dantas Palmeira J, Ferreira H, Madec JY, Haenni M. Pandemic Escherichia coli ST648 isolate harbouring fosA3 and blaCTX-M-8 on an IncI1/ST113 plasmid: A new successful combination for the spread of fosfomycin resistance? J Glob Antimicrob Resist. 2018;15:254-255. doi: 10.1016/j.jgar.2018.10.025.
57. Ewbank AC, Fuentes-Castillo D, Sacristán C, Esposito F, Fuga B, Cardoso B, Godoy SN, Zamana RR, Gattamorta MA, Catão-Dias JL, Lincopan N. World Health Organization critical priority Escherichia coli clone ST648 in magnificent frigatebird (Fregata magnificens) of an uninhabited insular environment. Front Microbiol. 2022;13:940600. doi: 10.3389/fmicb.2022.940600.
58. Pea F. Intracellular Pharmacokinetics of Antibacterials and Their Clinical Implications. Clin Pharmacokinet. 2018;57(2):177-189. doi: 10.1007/s40262-017-0572-y.
59. Pea F, Viale P, Furlanut M. Antimicrobial therapy in critically ill patients: a review of pathophysiological conditions responsible for altered disposition and pharmacokinetic variability. Clin Pharmacokinet. 2005;44(10):1009-34. doi: 10.2165/00003088-200544100-00002.

 doi:10.20944/preprints202508.0234.v1

60. Zigangirova NA, Zayakin ES, Kapotina LN, Kost EA, Didenko LV, Davydova DY, Rumyanceva JP, Gintsburg AL. Development of Chlamydial Type III Secretion System Inhibitors for Suppression of Acute and Chronic Forms of Chlamydial Infection. Acta Naturae. 2012;4(2):87-97.
61. Savitskii MV, Moskaleva NE, Brito A, Markin PA, Zigangirova NA, Soloveva AV, Sheremet AB, Bondareva NE, Lubenec NL, Tagliaro F, Tarasov VV, Tatzhikova KA, Appolonova SA. Pharmacokinetics, tissue distribution, bioavailability and excretion of the anti-virulence drug Fluorothiazinon in rats and rabbits. J Antibiot (Tokyo). 2024;77(6):382-388. doi: 10.1038/s41429-024-00719-1.
62. Zigangirova NA, Nesterenko LN, Sheremet AB, Soloveva AV, Luyksaar SI, Zayakin ES, Balunets DV, Gintsburg AL. Fluorothiazinon, a small-molecular inhibitor of T3SS, suppresses salmonella oral infection in mice. J Antibiot (Tokyo). 2021;74(4):244-254. doi: 10.1038/s41429-020-00396-w.
63. Garcia-Medina R, Dunne WM, Singh PK, Brody SL. Pseudomonas aeruginosa acquires biofilm-like properties within airway epithelial cells. Infect Immun. 2005;73(12):8298-305. doi: 10.1128/IAI.73.12.8298-8305.2005.
64. Høiby N. A short history of microbial biofilms and biofilm infections. APMIS. 2017;125(4):272-275. doi: 10.1111/apm.12686.
65. Hoiby N, Axelsen NH. Identification and quantitation of precipitins against Pseudomonas aeruginosa in patients with cystic fibrosis by means of crossed immunoelectrophoresis with intermediate gel. Acta Pathol Microbiol Scand B Microbiol Immunol. 1973;81(3):298-308. doi: 10.1111/j.1699-0463.1973.tb02207.x.
66. Burmølle M, Thomsen TR, Fazli M, Dige I, Christensen L, Homøe P, Tvede M, Nyvad B, Tolker-Nielsen T, Givskov M, Moser C, Kirketerp-Møller K, Johansen HK, Høiby N, Jensen PØ, Sørensen SJ, Bjarnsholt T. Biofilms in chronic infections - a matter of opportunity - monospecies biofilms in multispecies infections. FEMS Immunol Med Microbiol. 2010;59(3):324-36. doi: 10.1111/j.1574-695X.2010.00714.x.
67. Staudinger BJ, Muller JF, Halldórsson S, Boles B, Angermeyer A, Nguyen D, Rosen H, Baldursson O, Gottfreðsson M, Guðmundsson GH, Singh PK. Conditions associated with the cystic fibrosis defect promote chronic Pseudomonas aeruginosa infection. Am J Respir Crit Care Med. 2014;189(7):812-24. doi: 10.1164/rccm.201312-2142OC.
68. Voronina OL, Kunda MS, Ryzhova NN, Aksenova EI, Semenov AN, Lasareva AV, Amelina EL, Chuchalin AG, Lunin VG, Gintsburg AL. The Variability of the Order Burkholderiales Representatives in the Healthcare Units. Biomed Res Int. 2015;2015:680210. doi: 10.1155/2015/680210.
69. Wirth T, Falush D, Lan R, Colles F, Mensa P, Wieler LH, Karch H, Reeves PR, Maiden MC, Ochman H, Achtman M. Sex and virulence in Escherichia coli: an evolutionary perspective. Mol Microbiol. 2006 Jun;60(5):1136-51. doi: 10.1111/j.1365-2958.2006.05172.x.
70. Voronina OL, Kunda MS, Ryzhova NN, Aksenova EI, Sharapova NE, Semenov AN, Amelina EL, Chuchalin AG, Gintsburg AL. On Burkholderiales order microorganisms and cystic fibrosis in Russia. BMC Genomics. 2018;19(Suppl 3):74. doi: 10.1186/s12864-018-4472-9.
71. Prjibelski A, Antipov D, Meleshko D, Lapidus A, Korobeynikov A. Using SPAdes De Novo Assembler. Curr Protoc Bioinformatics. 2020;70(1):e102. doi: 10.1002/cpbi.102. PMID: 32559359.
72. Brettin, T., Davis, J.J., Disz, T., Edwards, R.A., Gerdes, S., Olsen, G.J., Olson, R., Overbeek, R., Parrello, B., Pusch, G.D., Shukla, M., Thomason, J.A. 3rd, Stevens, R., Vonstein, V., Wattam, A.R., Xia, F. RASTtk: a modular and extensible implementation of the RAST algorithm for building custom annotation pipelines and annotating batches of genomes. Sci Rep. 2015;5:8365. doi: 10.1038/srep08365.
73. Li, W., O'Neill, K.R., Haft, D.H., DiCuccio, M., Chetvernin, V., Badretdin, A. et al. RefSeq: expanding the Prokaryotic Genome Annotation Pipeline reach with protein family model curation. Nucleic Acids Res. 2021;49(D1):D1020-D1028. doi: 10.1093/nar/gkaa1105.
74. Liu B, Zheng D, Zhou S, Chen L, Yang J. VFDB 2022: a general classification scheme for bacterial virulence factors. Nucleic Acids Res. 2022;50(D1):D912-D917. doi: 10.1093/nar/gkab1107.
75. Kanehisa M, Sato Y, Morishima K. BlastKOALA and GhostKOALA: KEGG Tools for Functional Characterization of Genome and Metagenome Sequences. J Mol Biol. 2016;428(4):726-731. DOI: 10.1016/j.jmb.2015.11.006.

 doi:10.20944/preprints202508.0234.v1

76. Alcock BP, Huynh W, Chalil R, Smith KW, Raphenya AR, Wlodarski MA, et al. CARD 2023: expanded curation, support for machine learning, and resistome prediction at the Comprehensive Antibiotic Resistance Database. Nucleic Acids Res. 2023;51(D1):D690-D699. doi: 10.1093/nar/gkac920.
77. Olson RD, Assaf R, Brettin T, Conrad N, Cucinell C, Davis JJ, et al. Introducing the Bacterial and Viral Bioinformatics Resource Center (BV-BRC): a resource combining PATRIC, IRD and ViPR. Nucleic Acids Res. 2023;51(D1):D678-D689. doi: 10.1093/nar/gkac1003.
78. Naas T, Oueslati S, Bonnin RA, Dabos ML, Zavala A, Dortet L, Retailleau P, Iorga BI. Beta-lactamase database (BLDB) - structure and function. J Enzyme Inhib Med Chem. 2017;32(1):917-919. doi: 10.1080/14756366.2017.1344235.
79. Ross K, Varani AM, Snesrud E, Huang H, Alvarenga DO, Zhang J, Wu C, McGann P, Chandler M. TnCentral: a Prokaryotic Transposable Element Database and Web Portal for Transposon Analysis. mBio. 2021 Oct 26;12(5):e0206021. doi: 10.1128/mBio.02060-21.
80. Johansson MHK, Bortolaia V, Tansirichaiya S, Aarestrup FM, Roberts AP, Petersen TN. Detection of mobile genetic elements associated with antibiotic resistance in Salmonella enterica using a newly developed web tool: MobileElementFinder. J Antimicrob Chemother. 2021;76(1):101-109. doi: 10.1093/jac/dkaa390.
81. Carattoli A, Zankari E, García-Fernández A, Voldby Larsen M, Lund O, et al. In silico detection and typing of plasmids using PlasmidFinder and plasmid multilocus sequence typing. Antimicrob Agents Chemother. 2014;58(7):3895-903. doi: 10.1128/AAC.02412-14.
82. Wishart DS, Han S, Saha S, Oler E, Peters H, Grant JR, Stothard P, Gautam V. PHASTEST: faster than PHASTER, better than PHAST. Nucleic Acids Res. 2023;51(W1):W443-W450. doi: 10.1093/nar/gkad382.
83. Couvin D, Bernheim A, Toffano-Nioche C, Touchon M, Michalik J, Néron B, Rocha EPC, Vergnaud G, Gautheret D, Pourcel C. CRISPRCasFinder, an update of CRISRFinder, includes a portable version, enhanced performance and integrates search for Cas proteins. Nucleic Acids Res. 2018 Jul 2;46(W1):W246-W251. doi: 10.1093/nar/gky425. PMID: 29790974; PMCID: PMC6030898.
84. Alikhan NF, Petty NK, Ben Zakour NL, Beatson SA. BLAST Ring Image Generator (BRIG): simple prokaryote genome comparisons. BMC Genomics. 2011 Aug 8;12:402. doi: 10.1186/1471-2164-12-402.
85. Carver TJ, Rutherford KM, Berriman M, Rajandream MA, Barrell BG, Parkhill J. ACT: the Artemis Comparison Tool. Bioinformatics. 2005;21(16):3422-3. doi: 10.1093/bioinformatics/bti553.
86. Clermont O, Christenson JK, Denamur E, Gordon DM. The Clermont Escherichia coli phylo-typing method revisited: improvement of specificity and detection of new phylogroups. Environ Microbiol Rep. 2013;5(1):58-65. doi: 10.1111/1758-2229.12019.Tamura K, Stecher G, Kumar S. MEGA11: Molecular Evolutionary Genetics Analysis Version 11. Mol Biol Evol. 2021;38(7):3022-3027. doi: 10.1093/molbev/msab120.